chemiluminescent western system (Amersham) was used to detect secondary probes.

Statistical analysis

Data are expressed as mean ± s.d. The Student's *t*-test was used to compare differences. Statistical significance was defined when P was <0.05.

Acknowledgements

We thank Drs Tamotsu Yoshimori and Frank McCormick for providing pLC3-GFP plasmid and Onyx-015, respectively.

The study was supported by Grants-in-Aid from the Ministry of Education, Science and Culture, Japan; and Grants from the Ministry of Health and Welfare, Japan.

References

Aliberti J, Viola JP, Vieira-de-Abreu A, Bozza PT, Sher A, Scharfstein J. (2003). Bradykinin induces IL-12 production by dendritic cells: a danger signal that drives Th1 polarization. *J Immunol* **170**: 5349–5353.

Bartholomae WC, Rininsland FH, Eisenberg JC, Boehm BO, Lehmann PV, Tary-Lehmann M. (2004). T cell immunity induced by live, necrotic, and apoptotic tumor cells. *J Immunol* **173**: 1012–1022.

Glantzounis GK, Tsimoyiannis EC, Kappas AM, Galaris DA. (2005). Uric acid and oxidative stress. *Curr Pharm Des* **11**: 4145–4151.

Ho LJ, Wang JJ, Shaio MF, Kao CL, Chang DM, Han SW *et al.* (2001). Infection of human dendritic cells by dengue virus causes cell maturation and cytokine production. *J Immunol* **166**: 1499–1506.

Hu DE, Moore AM, Thomsen LL, Brindle KM. (2004). Uric acid promotes tumor immune rejection. *Cancer Res* **64**: 5059–5062.

Kawashima T, Kagawa S, Kobayashi N, Shirakiya Y, Umeoka T, Teraishi F *et al.* (2004). Telomerase-specific replication-selective virotherapy for human cancer. *Clin Cancer Res* **10**: 285–292.

Lenaerts L, Naesens L. (2006). Antiviral therapy for adenovirus infections. *Antiviral Res* **71**: 172–180.

Lindenmann J, Klein PA. (1967). Viral oncolysis: increased immunogenicity of host cell antigen associated with influenza virus. *J Exp Med* **126**: 93–108.

Manjili MH, Park J, Facciponte JG, Subjeck JR. (2005). HSP110 induces 'danger signals' upon interaction with antigen presenting cells and mouse mammary carcinoma. *Immunobiology* **210**: 295–303.

Shi Y, Evans JE, Rock KL. (2003). Molecular identification of a danger signal that alerts the immune system to dying cells. *Nature* **425**: 516–521.

Sijts A, Sun Y, Janek K, Kral S, Paschen A, Schadendorf D *et al.* (2002). The role of the proteasome activator PA28 in MHC class I antigen processing. *Mol Immunol* **39**: 165–169.

Steinman RM, Turley S, Mellman I, Inaba K. (2000). The induction of tolerance by dendritic cells that have captured apoptotic cells. *J Exp Med* **191**: 411–416.

Sun Y, Sijts AJ, Song M, Janek K, Nussbaum AK, Kral S *et al.* (2002). Expression of the proteasome activator PA28 rescues the presentation of a cytotoxic T lymphocyte epitope on melanoma cells. *Cancer Res* **62**: 2875–2882.

Taki M, Kagawa S, Nishizaki M, Mizuguchi H, Hayakawa T, Kyo S *et al.* (2005). Enhanced oncolysis by a tropism-modified telomerase-specific replication-selective adenoviral agent OBP-405 ('Telomelysin-RGD'). *Oncogene* **24**: 3130–3140.

Umeoka T, Kawashima T, Kagawa S, Teraishi F, Taki M, Nishizaki M *et al.* (2004). Visualization of intrathoracically disseminated solid tumors in mice with optical imaging by telomerase-specific amplification of a transferred green fluorescent protein gene. *Cancer Res* **64**: 6259–6265.

Watanabe T, Hioki M, Fujiwara T, Nishizaki M, Kagawa S, Taki M *et al.* (2006). Histone deacetylase inhibitor FR901228 enhances the antitumor effect of telomerase-specific replication-selective adenoviral agent OBP-301 in human lung cancer cells. *Exp Cell Res* **312**: 256–265.

Supplementary Information accompanies the paper on the Oncogene website (http://www.nature.com/onc).

Establishment of biological and pharmacokinetic assays of telomerase-specific replication-selective adenovirus

Yuuri Hashimoto,[1] Yuichi Watanabe,[1] Yoshiko Shirakiya,[1] Futoshi Uno,[2] Shunsuke Kagawa,[2] Hitoshi Kawamura,[1] Katsuyuki Nagai,[1] Noriaki Tanaka,[3] Horomi Kumon,[2] Yasuo Urata[1] and Toshiyoshi Fujiwara[2,4]

[1]Oncolys BioPharma, 3-16-33 Roppongi, Minato-ku, Tokyo 106-0031; [2]Center for Gene and Cell Therapy, Okayama University Hospital, 2-5-1 Shikata-cho, Okayama 700-8558; [3]Division of Surgical Oncology, Department of Surgery, Okayama University Graduate School of Medicine and Dentistry, 2-5-1 Shikata-cho, Okayama 700-8558, Japan

(Received June 25, 2007/Revised September 11, 2007/Accepted October 4, 2007/Online publication January 14, 2008)

The use of replication-selective tumor-specific viruses represents a novel approach for the treatment of neoplastic disease. We constructed an attenuated adenovirus, telomerase-specific replication-selective adenovirus (TRAD), in which the human telomerase reverse transcriptase promoter element drives the expression of the *E1A* and *E1B* genes linked with an internal ribosome entry site (IRES). Forty-eight hours after TRAD infection at a multiplicity of infection of 1.0, the cell viability of H1299 human lung cancer cells was consistently less than 50% and therefore this procedure could be used as a potency assay to assess the biological activity of TRAD. We also established a quantitative real-time polymerase chain reaction (PCR) analysis with consensus primers for either the adenovirus E1A or IRES sequence. The linear ranges of quantitation with E1A and IRES primers were 10^3–10^8 and 10^2–10^8 plaque-forming units/mL in the plasma, respectively. The PCR analysis demonstrated that the levels of *E1A* in normal tissues were more than 10^3 lower than in the tumors of A549 human lung tumor xenografts in *nu/nu* mice at 28 days after intratumoral injection. Our results suggest that the cell-killing assay against H1299 cells and real-time PCR can be used to assess the biological activity and biodistribution of TRAD in clinical trials. (*Cancer Sci* 2008; 99: 385–390)

The emerging fields of functional genomics and functional proteomics provide an expanding repertoire of clinically applicable targeted therapeutics.[1] Replication-selective oncolytic viruses provide a new platform for treatment of a variety of human cancers.[2,3] Promising clinical trials have shown the antitumor potency and safety of mutant or genetically modified adenoviruses.[4,5] We constructed previously an adenovirus vector, TRAD, in which the hTERT promoter element drives the expression of the *E1A* and *E1B* genes linked with an IRES. We showed that TRAD caused efficient selective killing of human cancer cells, but not normal cells.[6] Many studies have demonstrated that the majority of malignant tumors express telomerase activity,[7] suggesting that TRAD can potentially kill most human cancer cells.

TRAD can replicate and then lyse cancer cells, infect neighboring cancer cells, and subsequently induce oncolysis throughout the whole tumor mass *in vivo*. As preclinical models showed that TRAD could spread into the bloodstream, it is important to monitor carefully the amount of TRAD in the circulation after intratumoral injection of TRAD to avoid serious adverse events due to viremia. Although we used vector-specific primers that detected the p53 open reading frame–adenoviral DNA junction in a phase I clinical trial of a replication-deficient adenoviral vector expressing the wild-type *p53* gene (Advexin),[8] no appropriate method has been established to detect TRAD quantitatively. In addition, there is also a need for a procedure that can evaluate the biological activity of TRAD for clinical application.

In the present study, we characterized a potent antitumor viral agent, TRAD, to establish a biological assay and developed a single quantitative PCR method that can be used to assess the number of viral genomes present in the plasma as well as tissues.

Materials and Methods

Cells and culture conditions. H1299 (a human non-small-cell lung cancer cell line), H460 (a human large-cell lung cancer cell line), A549 (a human lung adenocarcinoma cell line), LNCap (a human metastatic prostate carcinoma cell line), MKN28 and MKN45 (human gastric adenocarcinoma cell lines), PC-3 (a human prostate adenocarcinoma cell line), SW620 (a human colorectal carcinoma cell line), and TE8 and T.Tn (human esophagus squamous carcinoma cell lines) were propagated to monolayer cultures in RPMI-1640 supplemented with 10% FBS, and 100 units/mL PG and 100 μg/mL SM. HeLa (a human cervical adenocarcinoma cell line), HepG2 (a human hepatocellular carcinoma cell line), Panc-1 (a human pancreatic epithelioid carcinoma cell line), and 293 (a transformed embryonic kidney cell line) were grown in DMEM containing high glucose (4.5 g/L) (high) with 10% FBS and PG/SM. HT-29 (a human colorectal adenocarcinoma cell line) was grown in McCoy's 5a with 10% FBS and PG/SM. MCF-7 (a human mammary gland adenocarcinoma cell line) was grown in Earle's Minimum Essential Medium with 10% FBS, PG/SM, and 2 mM L-glutamine. OST, SaOS2, and HOS (human osteosarcoma cell lines) were grown in DMEM (high) with 10% FBS and PG/SM. HSC-3 and HSC-4 (human tongue squamous carcinoma cell lines) were obtained from the Health Science Resources Bank (Osaka, Japan) and grown in DMEM (high) with 10% FBS and PG/SM. SCC-4 and SCC-9 (human tongue squamous carcinoma cell lines) were obtained from American Type Culture Collection (ATCC, Rockville, MD, USA) and grown in DMEM containing Nutrient Mixture (Ham's F-12) with 10% FBS, PG/SM, and 400 ng/mL hydrocortisone. U-2OS (a human osteosarcoma cell line) was obtained from ATCC and grown in McCoy's 5a with 10% FBS and PG/SM. NHLF was purchased from Takara Biomedicals (Kyoto, Japan) and cultured in the medium recommended by the manufacturer.

Recombinant adenoviruses. The recombinant replication-selective tumor-specific adenovirus vector TRAD was constructed and

[4]To whom correspondence should be addressed. E-mail: toshi_f@md.okayama-u.ac.jp
Abbreviations: ATCC, American Type Culture Collection; DMEM, Dulbecco's modified Eagle's medium; FBS, fetal bovine serum; hTERT, human telomerase reverse transcriptase; ID_{50}, the multiplicity of infection that causes 50% growth inhibition; IRES, internal ribosome entry site; NHLF, normal human lung fibroblasts; MOI, multiplicity of infection; PCR, polymerase chain reaction; PFU, plaque-forming units; PG, penicillin; SM, streptomycin; TRAD, telomerase-specific replication-selective adenovirus; XTT, sodium 3'-[1-(phenylaminocarbonyl)-3,4-tetrazolium]-bis(4-methoxy-6-nitro)benzene sulfonic acid hydrate.

doi: 10.1111/j.1349-7006.2007.00665.x

characterized as described previously.[6,9–11] The virus was purified by $CsCl_2$ step-gradient ultracentrifugation followed by $CsCl_2$ linear-gradient ultracentrifugation. The virus particle titer and infectious titer were determined spectrophotometrically and by plaque assay, respectively, in 293 cells.

Cell-viability assay. The XTT assay was carried out to measure cell viability. Cells were plated on 96-well plates at 1×10^3 cells/well 20 h before viral infection. HSC-4, SCC-4, and SCC-9 cells were then infected with TRAD at MOI of 0, 1, 10, and 50 PFU/cell. Other cell lines were infected with TRAD at MOI of 0, 0.1, 1, and 10 PFU/cell. Cell viability was determined at 1, 2, 3, and 5 days after virus infection using Cell Proliferation Kit II (Roche Molecular Biochemicals, Indianapolis, IN, USA) according to the protocol provided by the manufacturer. Using the cell viability data at 3 days after virus infection, we determined the TRAD ID_{50} of each cell line.

Cell-killing assay. H1299 cells were plated at 5×10^4 cells/well on 24-well plates and infected with TRAD at MOI of 0, 0.01, 0.1, 1, and 10 PFU/cell. Forty-eight hours later, the number of cells in each well was counted. Experiments were carried out in triplicate for each MOI, and cell viability was assessed by the trypan blue dye exclusion assay.

Quantitative real-time PCR assay. Viral DNA from serially diluted viral stocks and tumor cells infected with TRAD were extracted using QIAamp DNA Mini Kit (Qiagen, Valencia, CA, USA), and quantitative real-time PCR assay for either the *E1A* gene or the IRES sequence was carried out using a LightCycler instrument and a LightCycler DNA Master SYBR Green I kit (Roche Molecular Biochemicals). Typical amplification mixes (20 μL) contained 3 mM $MgCl_2$, 0.3 μM of each primer for IRES or 0.5 μM for *E1A*, and 2 μL of 10× LightCycler FastStart DNA Master SYBR Green I. The sequences of the specific primers used in this experiment were: IRES, 5′-GAT TTT CCA CCA TAT TGC CG-3′ and 5′-TTC ACG ACA TTC AAC AGA CC-3′; E1A, 5′-CCT GTG TCT AGA GAA TGC AA-3′ and 5′-ACA GCT CAA GTC CAA AGG TT-3′. PCR amplifications were carried out in glass capillary tubes. PCR amplification for IRES began with a 10-min denaturation step at 95°C and then 40 cycles of denaturation at 95°C for 10 s, annealing at 60°C for 10 s, and extension at 72°C for 6 s. PCR amplification for *E1A* began with a 10-min denaturation step at 95°C and then 40 cycles of denaturation at 95°C for 10 s, annealing at 58°C for 15 s, and extension at 72°C for 8 s. Data analysis was carried out using LightCycler Software (Roche Molecular Biochemicals).

***In vivo* human tumor model.** A549 human lung cancer cells (5×10^6 cells/mouse) were injected subcutaneously into the flank of 7- to 9-week-old female BALB/c *nu/nμ* mice and permitted to grow to approximately 5–6 mm in diameter. At that stage, a 100-μL solution containing 1×10^8 PFU of TRAD was injected into the tumor. The tumors and organs were harvested 28 and 70 days later and DNA was extracted from each tissue. To compare viral replication in the tumor and other normal organs, quantitative real-time PCR for the *E1A* gene was carried out using a LightCycler instrument. The experimental protocol was approved by the Ethics Review Committee for Animal Experimentation of Okayama University School of Medicine.

Statistical analysis. All data were expressed as mean ± SD. Differences between groups were examined for statistical significance using Student's *t*-test. A *P*-value less than 0.05 denoted the presence of a statistically significant difference.

Results

***In vitro* cytopathic efficacy of TRAD in human cancer cell lines derived from different organs.** To determine whether TRAD infection induces broad-spectrum selective cell lysis, 23 tumor cell lines derived from 11 different organs (head and neck, lung, esophagus, stomach, colon, liver, pancreas, breast, prostate, uterus, and bone) were infected with TRAD at various MOI. Previous studies using a real-time reverse transcription-PCR method have demonstrated that these cell lines express detectable levels of hTERT mRNA.[6,9] Cytotoxicity was then assessed using the XTT cell-viability assay over 5 days after infection. As shown in Figure 1a, TRAD infection induced cell death in all cell lines except T.Tn esophageal cancer cells in a dose-dependent manner. Calculated ID_{50} values confirmed that all cell lines except T.Tn could be killed efficiently by TRAD at an MOI of less than 25 (Fig. 1b). These results suggest the broad-spectrum antitumor potency of TRAD.

Establishment of a standard assay to assess the biological activity of TRAD. H1299 human lung cancer cells and LNCap human prostate cancer cells were the most sensitive cell lines to TRAD-induced cell death (Fig. 1b). Accordingly, we used H1299 cells to evaluate the biological activity of TRAD. To test whether the selective replication of TRAD translates into selective oncolysis, we compared the cytopathic effects of TRAD in H1299 cells and NHLF at 5 days after infection. The dose–response curve of the relative cell viability in H1299 cells was shifted to the left compared to that in NHLF, suggesting that TRAD killed H1299 cells 10^2–10^3 more efficiently than NHLF (Fig. 2a).

We next determined the minimal dose of TRAD that could induce more than 50% of cell death in H1299 cells. As shown in Figure 2b, the cell viability of H1299 cells was less than 40% at 48 h after their infection with TRAD at a MOI of 1.0, but was 60% after infection with a MOI of 0.1. We also confirmed that H1299 cells at various passages (5th to 20th after purchase from ATCC) could be killed by TRAD in a similar fashion (data not shown). Therefore, TRAD could be considered biologically active, if TRAD at a MOI of 1 reduces the cell viability of H1299 cells by more than 50% at 48 h after infection. To estimate the utility of this assay, we examined the biological activity of heat-inactivated TRAD. Infection with intact TRAD at a MOI of 10 induced approximately 90% reduction in H1299 cell viability at 48 h after infection, whereas the antitumor activity was completely inhibited when it was preheated at 56°C for 5 or 10 min (Fig. 2c).

Development of quantitative PCR assay to detect copy numbers of TRAD. We used real-time PCR for quantitative detection of TRAD. Oligonucleotide primers were designed to achieve DNA amplification of the adenoviral E1A or IRES sequences in the TRAD genome (Fig. 3a). To generate accurate standard curves, TRAD at a known concentration was serially diluted and used as a template for real-time PCR analysis. Detection of IRES and E1A genome copies was achieved consistently and reproducibly by the PCR cycle values used. A linear relationship could be obtained between the number of cycles and the $\log_{10}$ dilution when 10^2–10^8 IRES copies and 10^3–10^8 E1A copies were assayed. Regression analysis of IRES and E1A curves resulted in very high correlation coefficients (0.99 and 1.00, respectively) for these concentration ranges (Fig. 3b). In addition, the dilution of TRAD virus in the plasma did not affect the sensitivity and dynamic ranges of quantification (Fig. 3b), suggesting that this method can be used to detect TRAD in the blood circulation.

***In vitro* quantification and replication monitoring of TRAD in infected human tumor and normal cells.** We next examined the replication ability of TRAD in different cell lines by measuring the relative amounts of IRES and E1A copy numbers. LNCap and NHLF cells were harvested at the indicated time points over 5 and 7 days, respectively, after infection with TRAD, and subjected to quantitative real-time PCR analysis using IRES and E1A primers. The ratios were normalized by dividing the value of cells obtained at 2 h after viral infection. As shown in Figure 4a, TRAD replicated 10^3–10^4 by 5 days after infection; its replication, however, was attenuated to less than 10^1 in normal NHLF cells. We previously reported that TRAD could replicate 10^4–10^6 by 3 days after infection in H1299 cells;[6,10] however, as

doi: 10.1111/j.1349-7006.2007.00665.x

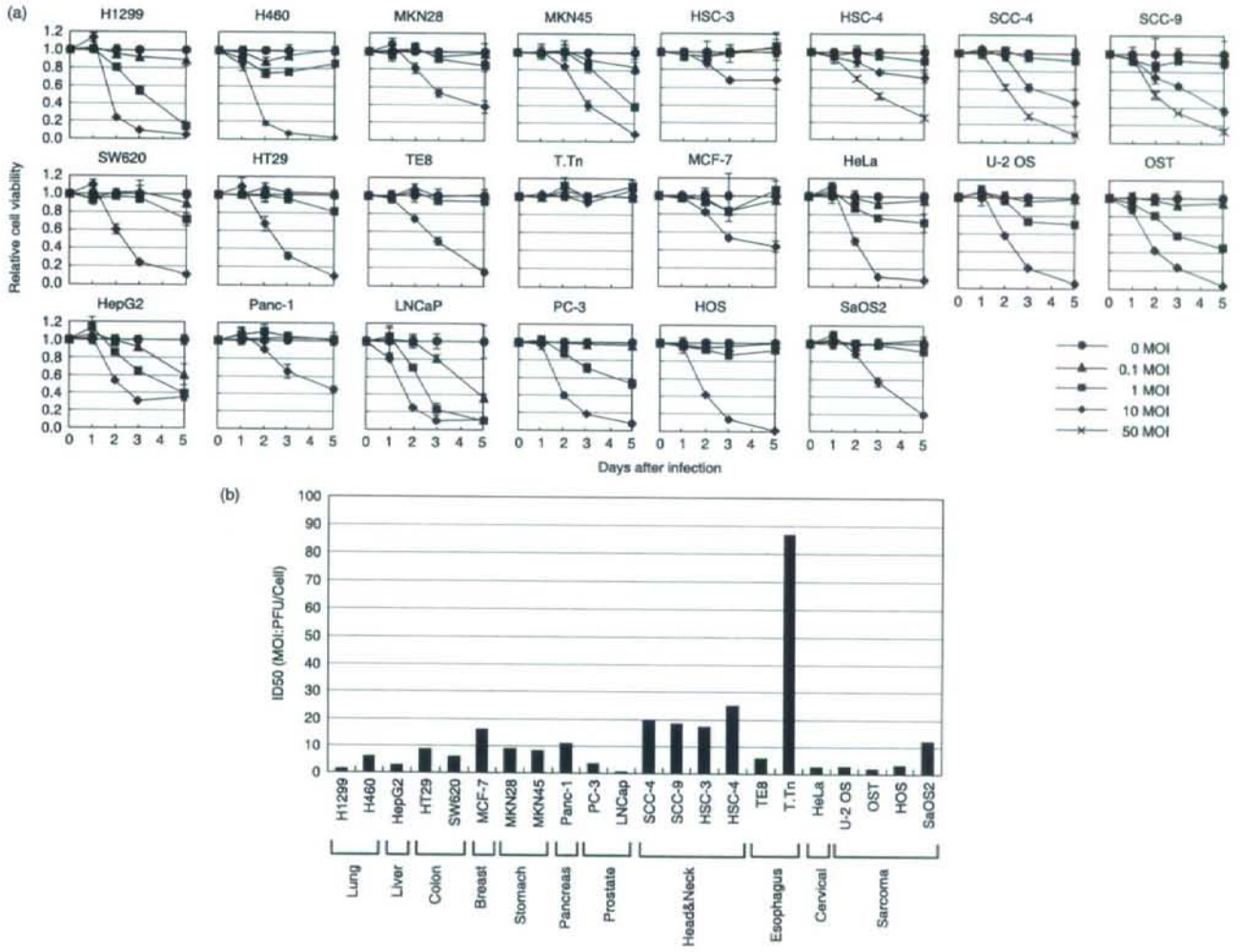

Fig. 1. Oncolytic effects of telomerase-specific replication-selective adenovirus (TRAD) *in vitro* on a variety of human cancer cell lines. (a) Cells were infected with TRAD at indicated multiplicity of infection (MOI) values, and surviving cells were quantitated over 5 days by XTT assay. Data are mean ± SD. (b) The 50% inhibiting doses of TRAD on cell viability at 3 days after infection were calculated and expressed as ID_{50} values. PFU, plaque-forming units; XXT, sodium 3'-[1-(phenylaminocarbonyl)-3,4-tetrazolium]-bis(4-methoxy-6-nitro)benzene sulfonic acid hydrate.

Cancer Sci | February 2008 | vol. 99 | no. 2 | 387

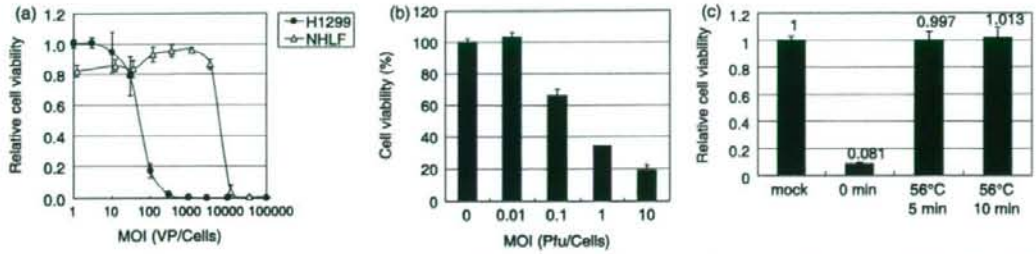

Fig. 2. Antitumor effects of telomerase-specific replication-selective adenovirus (TRAD) on H1299 non-small-cell lung cancer cells *in vitro*. (a) Effects of various concentrations of TRAD on H1299 cancer cells and normal human lung fibroblasts (NHLF) assessed at 5 days after treatment with XTT assay. Results are expressed as the percentage of untreated control. (b) H1299 cells were cultured as monolayers in triplicate in 24-well culture plates, infected with TRAD at the indicated multiplicities of infection (MOI), and assessed for cell viability 48 h after infection. Mock-infected cells were used as a control. (c) H1299 cells were plated on 96-well plates and infected with 10 MOI of TRAD heated at 56°C for 5 or 10 min, or non-treated TRAD. An XTT assay was carried out at 3 days after virus infection. Mock-infected cells were used as a control. Data represent the mean ± SD of triplicate experiments. PFU, plaque-forming units; XXT, sodium 3′-[1-(phenylaminocarbonyl)-3,4-tetrazolium]-bis(4-methoxy-6-nitro) benzene sulfonic acid hydrate; VP, virus particles.

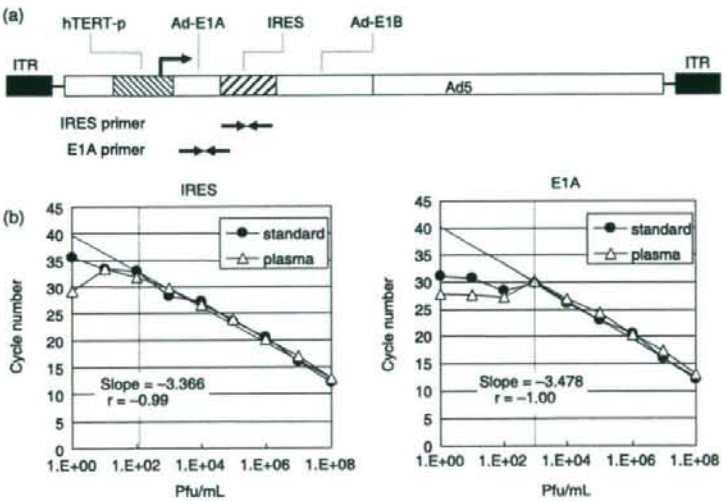

Fig. 3. Detection of normal human lung fibroblasts (TRAD) using quantitative polymerase chain reaction (PCR) assay. (a) Schematic diagram of the DNA structure of TRAD. TRAD contains the human telomerase reverse transcriptase (hTERT) promoter sequence inserted into the adenovirus genome to drive transcription of the *E1A* and *E1B* bicistronic cassette linked by the internal ribosome entry site (IRES) structure. Sites to which PCR primers (IRES and E1A) were targeted are indicated. Two primer pairs of IRES and E1A were designed to detect the TRAD genome. (b) Standard calibration curves of threshold cycle values and copy numbers are shown using serial dilution of TRAD virus stock. The coefficient of correlation (r^2) and slope are indicated for assays with IRES and E1A primers. ITR, inverted terminal repeats; PFU, plaque-forming units.

LNCap cells were more sensitive to TRAD-mediated cytotoxicity than H1299 cells (Fig. 1a), viral replication reached a plateau phase around 10^4 when LNCap cells started to die. Moreover, PCR targeting IRES and E1A showed similar replication profiles for TRAD in MCF-7 human breast cancer cells (Fig. 4b). To monitor the long-term viral replication, MCF-7 cells that were less sensitive to the cytopathic effect of the virus were used.

***In vivo* determination of TRAD genomes in tissue samples after intratumoral injection.** To evaluate selective replication of TRAD *in vivo*, we examined mouse tissues, including implanted tumors, for the presence of viral DNA by quantitative real-time PCR, following intratumoral viral injection. Mice with established subcutaneous A549 human lung tumor xenografts received a single intratumoral injection of 1×10^8 PFU of TRAD, and were killed 28 or 70 days after injection. To obtain the sufficient amounts of tumor tissues for analysis, we chose to use A549 cells. Our preliminary experiments demonstrated that intratumoral administration of TRAD suppressed tumor growth significantly compared with mock-treated tumors at 42 days after initiation of treatment ($P < 0.05$); however, the *in vivo* antitumor effect against A549 tumors was less than that against H1299 or LNCap tumors (data not shown). Although E1A DNA was detected in serum and some normal tissues examined (brain, heart, lung, ovary, liver, uterus, kidneys, bladder, colon, and axillary and mesenteric lymph nodes), tumors injected with TRAD contained at least 1000-fold more *E1A* copies (Fig. 5). These results suggest that quantitative real-time PCR allows detection and quantification of the number of TRAD genomes present in tissue samples after intratumoral injection of TRAD *in vivo*.

Discussion

Oncolytic viruses have been developed as anticancer agents based on the advantage of selective killing of tumor cells by controlled replication of the virus in the tumors, resulting in minimal undesired effects on normal cells.[2] Furthermore, amplified viruses can infect adjacent tumor cells as well as reach distant metastatic tumors through the blood circulation. Alhtough this might be a potential advantage of oncolytic viruses, systemic dissemination of large amounts of virus may induce virus-related symptoms including fever, diarrhea, pneumonia, and hepatitis, eventually leading to death. Therefore, virus shedding and distribution have to be evaluated by appropriate and suitable methods. In addition,

doi: 10.1111/j.1349-7006.2007.00665.x

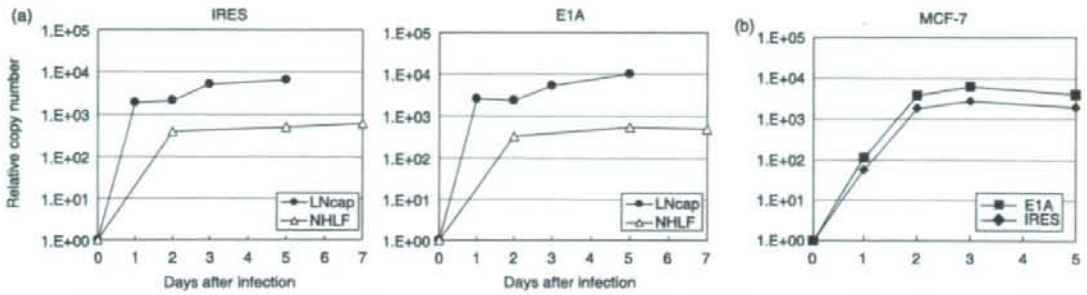

Fig. 4. Quantitative measurement of viral DNA replication in human cancer and normal cells *in vitro* by quantitative polymerase chain reaction (PCR) assay. (a) LNCap human prostate cancer cells and normal human lung fibroblast (NHLF) cells were infected with telomerase-specific replication-selective adenovirus (TRAD) at a multiplicity of infection (MOI) of 1 for 2 h. Following the removal of virus inoculum, cells were further incubated for the indicated periods of time, and then subjected to the real-time quantitative PCR assay. The amounts of viral internal ribosome entry site (IRES) and E1A copy number was defined as the fold increase for each sample relative to that at 2 h (2 h equals 1). (b) MCF-7 human breast cancer cells were infected with TRAD at a MOI of 1 and subjected to the PCR assay at the indicated time points. The relative TRAD DNA levels detected by IRES and E1A primers were plotted.

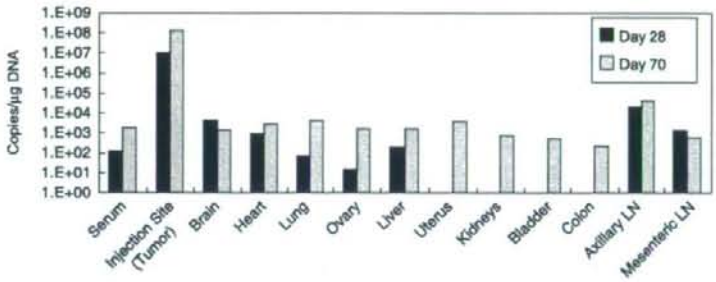

Fig. 5. Spread and replication of telomerase-specific replication-selective adenovirus (TRAD) following intratumoral administration in *nu/nu* mice transplanted with A549 tumor cells. A549 tumor cells were injected subcutaneously into the right flank of mice at 5×10^6 cells/mouse. Mice received intratumoral injection of 1×10^8 plaque-forming units of TRAD when the tumor reached a size of approximately 5–6 mm in diameter. DNA was extracted from the subcutaneous tumor and various tissues of *nu/nu* mice at 28 or 70 days after infection. Viral DNA was detected by quantitative polymerase chain reaction amplification of the adenoviral E1A sequence. The amounts of TRAD genome were defined as viral E1A copy number per μg DNA. LN, lymph nodes.

to avoid unexpected infectious disease due to viral overdose, we need assays that accurately detect the biological activity of viruses. In the present study, for clinical trials of TRAD, we developed an assay designed to estimate the biological activity of TRAD and to detect the copy number of TRAD in the plasma as well as tissues.

Although telomerase-specific TRAD exhibited a broad cytopathic effect against human cancer cell lines of different tissue origins, a human non-small-cell lung cancer cell line, H1299, was chosen for the biological assay of TRAD. H1299 was one of the most sensitive cell lines to TRAD-mediated cell death (ID_{50} = 0.94 MOI) and could be killed efficiently by TRAD infection in a dose-dependent fashion (Fig. 1). Because H1299 cells can be obtained from ATCC, they can be used in clinical laboratories to assess the biological activity of TRAD with a qualified standard protocol. In addition, although adenoviral E1B-55 kDa protein is known to bind to the tumor suppressor p53 protein,[12] H1299 cells are p53-null and therefore the interaction of E1B-55 kDa with p53, which in turn results in transcriptional modulation, can be ignored in this cell line. Thus, H1299 is considered an appropriate cell line for assessment of TRAD activity in certain preparations. In the present study, we considered TRAD to be active when the viability of H1299 cells was reduced by more than 50% at 48 h after TRAD infection at an MOI of 1. Using this biological assay, we confirmed that heat treatment of aliquots of TRAD at 56°C for 5 min is sufficient to inactivate its antitumor potential (Fig. 2c). These results advocate the use of the H1299 cell-based cytotoxicity assay as a standard method for quantitative assessment of the biological activity of TRAD in virus stocks for clinical trials.

Various biological methods, such as determination of infectious units in plaque assays, have been used routinely in clinical trials to monitor viral loads in the peripheral circulation.[8] These methods are useful for evaluating safety because the viral titers directly reflect the infectivity of viruses. However, because the plaque assay consists of labor-intensive and time-consuming steps, real-time monitoring of the biodistribution of the virus might be difficult. Here we described the development of a quantitative real-time PCR assay that can accurately quantify genome copy numbers of TRAD over a large linear range. Using primers targeting TRAD-specific sequences, such as adenoviral E1A and IRES, real-time PCR could accurately detect the number of TRAD genomes in the plasma as well as in the cells (Figs 3,4). The assay showed that TRAD replicated even in NHLF, although the level was much lower than that in tumor cells. It is usually difficult to maintain the normal cells primarily isolated from human tissues such as human hepatocytes in the culture; however, commercially available NHLF could be cultured for several passages, suggesting that NHLF may have some characteristics different from primary isolated normal cells, including

telomerase activity. We also found that the number of viral genomes could be measured in genomic DNA purified from tissues of mice *in vivo* after injection of TRAD into the xenografts (Fig. 5). Although viral DNA could be detected even in normal tissues 70 days after intratumoral injection of TRAD, the absence of infectious virus as assessed by the plaque assay suggests that there are only DNA fragments in tissues. Our preliminary experiments have demonstrated that DNA could be isolated from tumors as small as 5 mm in diameter (data not shown). Therefore, the real-time PCR method with E1A and IRES primers permits rapid and quantitative detection of TRAD DNA in clinical samples.

We have shown recently the antiviral activity of cidofovir against TRAD *in vitro*. Cidofovir is an acyclic nucleoside phosphonate with potent broad-spectrum anti-DNA viral activity and has been approved for the treatment of many types of viruses, including cytomegalovirus and adenovirus.[13] Although viremia after TRAD administration is extremely rare because of the anti-adenovirus antibodies expected to be present in most patients, a real-time PCR-based pharmacokinetic assay can allow the early detection of disseminated virus, and thus its use could provide an indication for commencement of cidofovir treatment in clinical trials.

In summary, we have established a fast, reliable, and sensitive assay to assess the biological activity of TRAD *in vitro* and to detect the viral genome in the plasma as well as tissues *in vivo*. A phase I clinical trial of TRAD targeting advanced solid tumors is currently underway in the USA following the approval of the Food and Drug Administration. Such an assay has been used in this ongoing trial and the data will be analyzed in the near future for the assessment of the safety, efficacy, and biodistribution of TRAD.

Acknowledgments

This work was supported in part by grants from the Ministry of Education, Science, and Culture, Japan, and by grants from the Ministry of Health and Welfare, Japan.

References

1 Kohn EC, Lu Y, Wang H *et al.* Molecular therapeutics: promise and challenges. *Semin Oncol* 2004; **31**: 39–53.
2 Hawkins LK, Lemoine NR, Kirn D. Oncolytic biotherapy: a novel therapeutic platform. *Lancet Oncol* 2002; **3**: 17–26.
3 Chiocca EA. Oncolytic viruses. *Nat Rev Cancer* 2002; **2**: 938–50.
4 Reid T, Galanis E, Abbruzzese J *et al.* Hepatic arterial infusion of a replication-selective oncolytic adenovirus (dl1520): phase II viral, immunologic, and clinical endpoints. *Cancer Res* 2002; **62**: 6070–9.
5 Hamid O, Varterasian ML, Wadler S *et al.* Phase II trial of intravenous CI-1042 in patients with metastatic colorectal cancer. *J Clin Oncol* 2003; **21**: 1498–504.
6 Kawashima T, Kagawa S, Kobayashi N *et al.* Telomerase-specific replication-selective virotherapy for human cancer. *Clin Cancer Res* 2004; **10**: 285–92.
7 Kim NW, Piatyszek MA, Prowse KR *et al.* Specific association of human telomerase activity with immortal cells and cancer. *Science* 1994; **266**: 2011–15.
8 Fujiwara T, Tanaka N, Kanazawa S *et al.* Multicenter phase I study of repeated intratumoral delivery of adenoviral p53 in patients with advanced non-small-cell lung cancer. *J Clin Oncol* 2006; **24**: 1689–99.
9 Umeoka T, Kawashima T, Kagawa S *et al.* Visualization of intrathoracically disseminated solid tumors in mice with optical imaging by telomerase-specific amplification of a transferred green fluorescent protein gene. *Cancer Res* 2004; **64**: 6259–65.
10 Taki M, Kagawa S, Nishizaki M *et al.* Enhanced oncolysis by a tropism-modified telomerase-specific replication-selective adenoviral agent OBP-405 ('Telomelysin-RGD'). *Oncogene* 2005; **24**: 3130–40.
11 Watanabe T, Hioki M, Fujiwara T *et al.* Histone deacetylase inhibitor FR901228 enhances the antitumor effect of telomerase-specific replication-selective adenoviral agent TRAD in human lung cancer cells. *Exp Cell Res* 2006; **312**: 256–65.
12 Cathomen T, Weitzman MD. A functional complex of adenovirus proteins E1B-55kDa and E4orf6 is necessary to modulate the expression level of p53 but not its transcriptional activity. *J Virol* 2000; **74**: 11 407–12.
13 Ouchi M, Kawamura H, Nagai K, Urata Y, Fujiwara T. Antiviral activity of cidofovir against telomerase-specific replication-competent adenovirus, Telomelysin (OBP-301). *Mol Ther* 2007; **15** (Suppl 1): S173.

doi: 10.1111/j.1349-7006.2007.00665.x

Int. J. Cancer: **122,** 2628–2633 (2008)

Combination of oncolytic adenovirotherapy and Bax gene therapy in human cancer xenografted models. Potential merits and hurdles for combination therapy

Masayoshi Hioki[1,2], Shunsuke Kagawa[1,2]*, Toshiya Fujiwara[1,2], Ryo Sakai[1,2], Toru Kojima[1,2], Yuichi Watanabe[1,3], Yuuri Hashimoto[3], Futoshi Uno[1,2], Noriaki Tanaka[1] and Toshiyoshi Fujiwara[1,2]

[1]*Division of Surgical Oncology, Department of Surgery, Okayama University Graduate School of Medicine, Dentistry and Pharmaceutical Sciences, 2-5-1 Shikata-cho, Okayama 700-8558, Japan*
[2]*Center for Gene and Cell Therapy, Okayama University Hospital, Okayama, Japan*
[3]*Oncolys BioPharma, Inc., Tokyo, Japan*

Cancer gene therapy and oncolytic virotherapy have been studied extensively. However, their clinical application is hampered by their weak anticancer activity. We previously constructed a replicating adenovirus (OBP-301, Telomelysin), in which the human telomerase reverse transcriptase (hTERT) promoter drives expression of the adenoviral E1 genes, and causes selective lysis of human cancer cells. We hypothesized that combination adenoviral therapy containing OBP-301 and a nonreplicating adenovirus expressing the proapoptotic Bax gene could overcome the weakness and augment the anticancer efficacy of each modality. Combination treatment resulted in marked Bax protein expression and enhanced efficacy in *in vitro* cell viability assay, when compared with either single treatment. However, combination treatment was not as effective in suppressing both subcutaneous and pleural disseminated tumors compared with OBP-301 treatment alone. Further investigation revealed that combination treatment resulted in suppressed E1A protein expression associated with reduced viral replication. Our results suggest that Bax gene therapy in combination with oncolytic adenovirotherapy potentially augments their antitumor activity, but further improvements may be required to maximize the combinatorial effect *in vivo*, for the Bax gene expression to avoid interference with production of the oncolytic virus.

Key words: gene therapy; oncolytic virus; bax; adenovirus

Oncolytic adenoviruses that can selectively replicate in tumor cells and cause lysis of infected cells have been extensively investigated as novel anticancer agents.[1,2] Recently, such vectors have been approved for clinical trials.[3–8] However, preclinical and clinical studies have revealed that the clinical application of these agents is hampered by their weak anticancer activity. Therefore, the development of strategies that maximize their anticancer activity is essential to the success of these agents in treating cancer.

One of the approaches to overcome this weakness is combination therapy of the oncolytic virus with a virus expressing therapeutic genes such as proapoptotic genes to augment the killing effect on cancer cells, which may lead to the future development of an arming oncolytic virus as a cancer therapeutic.

Bax is a strong proapoptotic gene that causes cytochrome C release from mitochondria, activates the caspase pathway and leads to apoptosis.[9,10] We previously constructed a binary adenoviral vector system (Ad/PGK-GV16 + Ad/GT-Bax: Ad/Bax) for Bax overexpression[11] that can transfer the Bax gene to cancer cells *in vitro* and *in vivo* and induce effective apoptosis.[12,13] However, because this system consists of E1-deleted, replication-defective adenovirus, its cell killing activity is theoretically limited to the transduced cells.

We also constructed a novel oncolytic adenovirus (OBP-301, Telomelysin), in which the human telomerase reverse transcriptase (hTERT) promoter drives expression of the adenoviral E1 genes. OBP-301 thus replicates preferentially in human cancer cells and causes their selective lysis.[14] However, as this virus also does not contain any therapeutic genes, clinical weakness is anticipated.

We hypothesize that Bax gene therapy in combination with an onlytic adenovirus could augment anticancer efficacy by overcoming the weakness of each modality. The replication-defective adenovirus with E1 deletion can become replication-competent when cotransduced with an oncolytic adenovirus supplying E1 *in trans*. Thus, the expression of the Bax gene and the viral copies would increase, which facilitates cancer cells to undergo apoptosis, release virus progenies and further spread them within the tumor.

In this study, we evaluated the transgene expression, viral replication and antitumor effect of Bax gene therapy combined with OBP-301 oncolytic adenovirotherapy in human cancer cell lines.

Material and methods

Cell lines and cell culture

Human bronchioloalveolar carcinoma A549 cells were propagated in a monolayer culture in Dulbecco's modified Eagle's medium containing Ham's F-12 nutrient mixture supplemented with 10% fetal calf serum (FCS) and antibiotics. Human gastric cancer MKN45 cells were cultured in RPMI 1640 medium containing 10% FCS and antibiotics. The cells were cultured at 37°C in a humidified incubator containing 5% CO_2.

Recombinant adenoviruses

The recombinant replication-selective, tumor-specific adenovirus vector OBP-301 (Telomelysin), and nonreplicating E1-deleted binary adenovirus vector system expressing the proapoptotic Bax gene (Ad/PGK-GV16 + Ad/GT-Bax: Ad/Bax) were previously constructed and characterized.[11,14] In a binary vector system, expression of the *Bax* gene can be induced by transferring Ad/GT-Bax into target cells along with Ad/PGK-GV16 at a ratio of 1:1. All of the viruses were propagated in a package containing 293 cells and purified by $CsCl_2$ step gradient ultracentrifugation followed by $CsCl_2$ linear gradient ultracentrifugation. Determination of virus particle titer and infectious titer (plaque-forming unit: PFU) was accomplished spectrophotometrically by the method of Maizel *et al.*[15] and by the method of Kanegae *et al.*,[16] respectively. The particles: plaque ratios were between 23:1 and 35:1.

Cell viability assay

Cells were plated in 96-well plates at a density of 1,000 cells/well and infected with OBP-301 alone, Ad/Bax alone, or their combination 15 hr later. Cell viability was assessed using a colorimetric XTT assay with the Cell Proliferation Kit II (Roche Molecular Biochemicals, Indianapolis, IN) according to the manufacturer's protocol. We determined the combination index (CI) at

This article contains supplementary material available via the Internet at http://www.interscience.wiley.com/jpages/0020-7136/suppmat.

Grant sponsors: Ministry of Education, Culture, Sports, Science and Technology of Japan, Ministry of Health, Labour and Welfare of Japan.

***Correspondence to:** Center for Gene and Cell Therapy, Okayama University Hospital, 2-5-1 Shikata-cho, Okayama 700-8558, Japan.
Fax: +81-86-235-7884. E-mail: skagawa@md.okayama-u.ac.jp

Received 8 May 2007; Accepted after revision 5 December 2007
DOI 10.1002/ijc.23438
Published online 13 March 2008 in Wiley InterScience (www.interscience.wiley.com).

different multiplicities of infection (MOIs) in A549 cells with CalcuSyn software (BioSoft, Cambridge, UK).

Cell cycle analysis

A549 and MKN45 cells were seeded on 6-well plates at 1×10^5 cells/well and were infected with OBP-301 at an MOI of 1 PFU/cell, Ad/Bax at an MOI of 5 or 50 PFU/cell, or OBP-301 at an MOI of 1 PFU/cell in combination with Ad/Bax at an MOI of 5 PFU/cell 15 hr later. At 24 and 96 hr after infection, adherent cells were harvested with trypsin-EDTA and nonadherent cells were also harvested. All cells were washed with PBS, fixed and permeated with 70% ice-cold ethanol at 4°C for 12 h. Cells were centrifuged at 1,200 rpm, resuspended in freshly prepared propidium iodide (PI) staining buffer (0.1% Triton X-100, 200 μg/ml RNase, and 50 μg/ml PI in PBS), and incubated for 30 min at 4°C in the dark. Single color fluorescent flow cytometry was performed with a FACS calibur flow cytometer (Becton Dickinson, San Jose, CA). The histograms were analyzed with FlowJO software (Tree Star, Ashland, OR).

Western blot analysis

A549 cells were seeded and infected with OBP-301 alone, Ad/Bax alone, or their combination at an MOI of 1 PFU/cell 15 hr later. The cells were incubated at 37°C and harvested for Western blot analysis at 72 and 120 hr. The primary antibodies against Bax (Santa Cruz Biotechnology, Santa Cruz, CA), caspase 3, E1A (BD Biosciences, San Jose, CA) and β-actin (Sigma, St. Louis, MO) and peroxidase-linked secondary antibody (Amersham, Arlington Heights IL) were used. Cells were washed twice in cold PBS, collected and lysed in lysis buffer [10 mM Tris (pH 7.5), 150 mM NaCl, 50 mM NaF, 1 mM EDTA, 10% glycerol, 0.5% NP40] containing proteinase inhibitors (0.1 mM phenylmethylsulfonyl fluoride, 0.5 mM Na3VO4). After 20 min on ice, the lysates were spun at 14,000 rpm at 4°C for 10 min. The supernatants were used as whole cell extracts. Protein concentration was determined using the Bio-Rad protein determination method (Bio-Rad, Richmond, CA). Equal amounts of proteins were boiled for 5 min and electrophoresed under reducing conditions on 4–12% (w/v) polyacrylamide gels. Proteins were electrophoretically transferred to Hybond polyvinylidene difluoride transfer membranes (Amersham Life Science, Buckinghamshire, UK) and incubated with the primary followed by peroxidase-linked secondary antibody. An ECL chemiluminescent Western blot system (Amersham) was used to detect secondary probes.

Animal experiments

A549 xenografts were established in 6-week-old female nude mice (Balb/c nu/nu) through subcutaneous inoculation of 2×10^6 A549 cells into the dorsal flank. Once each tumor reached a diameter of ~3–9 mm, the mice were randomly assigned into 4 groups and a 50-μl solution containing OBP-301, Ad/Bax, or their combination, at a dose of 1×10^7 PFU/body or PBS was injected into the tumor on 3 consecutive days. Tumors were measured 2–3 times a week and tumor volume was calculated using the equation $a \times b^2 \times 0.5$, in which a and b are the largest and smallest diameters, respectively. Animals were killed when their tumor reached a diameter of ~15 mm. To develop pleural disseminated xenografts, mice were inoculated with 2×10^6 A549 cells into the pleural cavity through a 27-gauge needle. Also, to assess the efficiency of adenoviral gene transfer into the pleural disseminated tumors, 24 hr after tumor injection, 100 μl of 1.0×10^7 PFU of OBP-301, Ad/Bax, both of them, or PBS was injected into the thoracic space by the same technique. The procedure was repeated over 3 consecutive days. Three weeks after cell inoculation, the mice were killed and their thoracic spaces were examined macroscopically for any growths. Tumors in the thoracic spaces were removed and weighed. The experimental protocol was approved by the Ethics Review Committee for Animal Experimentation of Okayama University School of Medicine, Okayama, Japan. The tumor growth of each group was statistically analyzed by Student t-test and a p-value of ≤ 0.05 was considered significant.

Viral replication assay in vivo

A549 cells were injected into the dorsal flank of nude mice. When the tumor reached a size of ~5 mm, 1×10^7 PFU of OBP-301, OBP-301 + Ad/Bax, OBP-301 + Ad/LacZ, or Ad/Bax was injected to the tumors ($n = 5$, each group). Tumors were harvested 7 days after viral injection, immediately frozen and milled in PBS by using Micro Smash MS-100 (Tomy Digital Biology, Tokyo, Japan). The virus was then extracted by freezing and thawing 3 times and cell debris was spun down. The supernatant was collected and subjected to titer assay for viral PFU. The final result was expressed as a total PFU from 1 whole tumor.

Quantitative real-time polymerase chain reaction

A549 cells were seeded on 25-cm^2 flasks at 5×10^5 cells 15 hr before infection. Cells were infected with OBP-301 alone or in combination with Ad/Bax or Ad/lacZ 15 hr later. The cells were incubated at 37°C, trypsinized and harvested for replication analysis at 48 hr. DNA purification was performed using a QIAmp DNA mini kit (Qiagen, Valencia, CA). The E1A DNA copy number was determined by quantitative real time polymerase chain reaction (PCR), using a LightCycler instrument and LightCycler-DNA Master SYBR Green I (Roche Diagnostics).

Results

Combination of oncolytic virotherapy and Bax gene therapy enhanced cell killing in vitro

To compare the efficacy of the combined use of oncolytic virotherapy with Bax gene therapy *in vitro*, A549 and MKN45 human cancer cells were treated with OBP-301 alone, Ad/Bax alone, or the combination. Based on each optimal condition, A549 was infected with OBP-301 at 1 MOI and Ad/Bax at 10 MOI, and MKN45 was infected at 10 MOI in both viruses. In both cell lines, Ad/Bax treatment showed only minimal suppression of cell viability and OBP-301 treatment showed a modest and delayed oncolytic effect, whereas combination treatment with OBP-301 and Ad/Bax induced rapid and massive cell death, and almost complete cell killing (Fig. 1).

To evaluate the synergistic effect of the combined oncolytic virotherapy and Bax gene therapy, the CI was determined at different MOIs (Table I) with CalcuSyn software (BioSoft, Cambridge, UK). We found that in A549 cells, the combination of OBP-301 with Ad/Bax led to a strong synergism (CI < 0.3).

Bax gene therapy in combination with oncolytic virotherapy increased the production of Bax protein in vitro *and induction of apoptosis*

To examine Bax protein expression in cells infected with the replication-deficient Ad/Bax in combination with the replicating OBP-301, A549 cells were infected with OBP-301 alone, Ad/Bax alone, or OBP-301 in combination with Ad/Bax or Ad/lacZ and then harvested on day 3 or 5. Cells treated with OBP-301 or the combination of OBP-301 with Ad/lacZ resulted in minimal Bax protein expression, whereas treatment with Ad/Bax and the combination treatment with OBP-301 plus Ad/Bax showed higher expression of Bax protein. Densitometric measurement documented increments of Bax expression by combination of Ad/Bax with OBP-301 (Fig. 2). In addition, treatment with OBP-301 plus Ad/Bax resulted in caspase-3 activation, while treatment with OBP-301 only or OBP-301 plus control virus Ad/lacZ did not. This means that the combination with Ad/Bax activates the apoptotic cascade in cancer cells cotreated with oncolytic virus.

Bax gene therapy in combination with oncolytic virotherapy increased apoptotic cells in vitro

To quantify the apoptotic effects of Ad/Bax treatment in combination with OBP-301 treatment, sub-G1/G0 fractions were

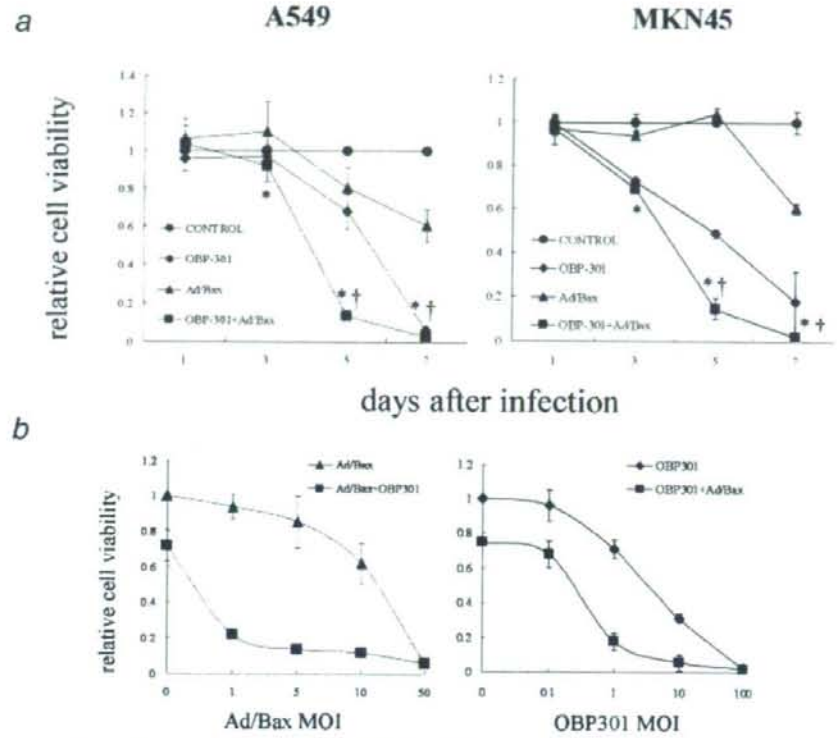

FIGURE 1 – Cytotoxity effects of OBP-301 combined with Ad/Bax in human cancer cell lines. (*a*) The indicated cancer cells were infected with OBP-301 alone, Ad/Bax alone, or in combination at the indicated MOI. Cell viability was assessed by XTT assay over 7 days. Bars, standard deviation (SD). *, $p < 0.05$, OBP-301 + Ad/Bax versus Ad/Bax alone; †, $p < 0.05$, OBP-301 + Ad/Bax versus OBP-301 alone. (*b*) A549 cells were infected with 1 MOI of OBP-301 and Ad/Bax at the indicated MOI (left), or 10 MOI of Ad/Bax and OBP-301 at the indicated MOI (right). Cell viability was assessed by XTT assay at 5 days after infection. Bars, SD.

TABLE I – COMBINATION INDEX (CI) OF OBP-301 AND Ad/Bax

Ad/Bax (MOI)	CI
1	0.122
5	0.111
10	0.132
50	0.217
OBP301 (MOI)	**CI**
0.1	1.054
1	0.144
10	0.197
100	0.592

determined by flow cytometry. A549 cells were infected with OBP-301, Ad/Bax, or OBP-301 plus Ad/Bax, and then subjected to the analysis at day 4. Although treatment with OBP-301 or Ad/Bax resulted in only background levels of apoptotic cells similar to that of mock infection, treatment with Ad/Bax plus OBP-301 markedly increased the apoptotic cells (Fig. 3).

Combination with Bax gene therapy did not augment antitumor activity of OBP-301-mediated oncolytic virotherapy in vivo

Based on the *in vitro* favorable combination effect of Ad/Bax and OBP-301, the antitumor effect on established tumors was further assessed. The A549 tumors were established in the dorsal

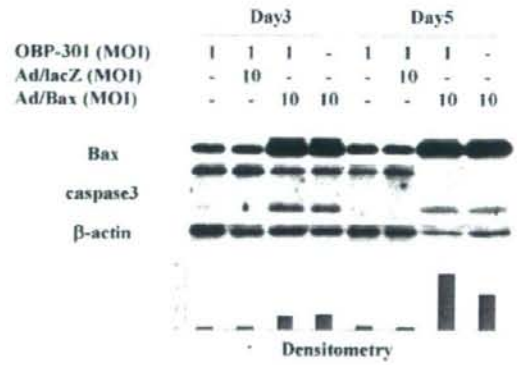

FIGURE 2 – Expression of Bax and caspase 3 in cells infected with Ad/Bax in combination with OBP-301. A549 cells were infected at 1 MOI of OBP-301 alone, 10 MOI of Ad/Bax alone, or 1 MOI of OBP-301 in combination with 10 MOI of Ad/Bax or Ad/lacZ, and then harvested at day 3 or 5. Lysates were subjected to immunoblot analysis with antibodies recognizing Bax, caspase 3, or β-actin. The lower panel shows the intensity of each band of Bax determined by densitometric scanning using NIH image software and normalized by dividing the actin signal.

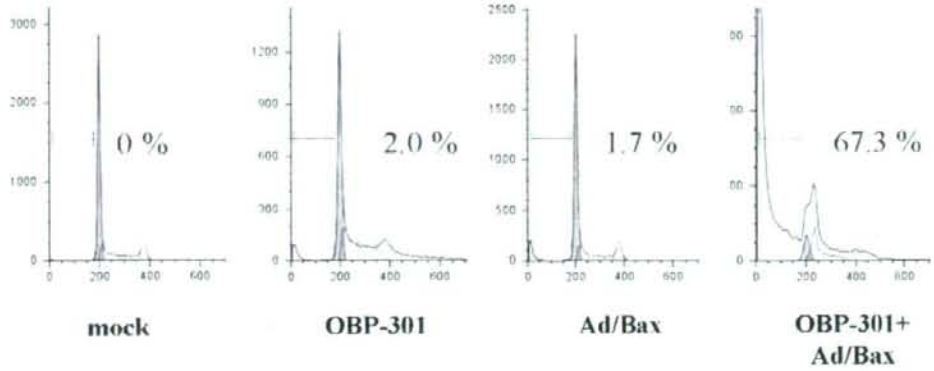

FIGURE 3 – Cell cycle analysis in A549 cells infected with OBP-301 in combination with Ad/Bax. Indicated cancer cells were infected with mock solution, 1 MOI of OBP-301, 10 MOI of Ad/Bax, or 1 MOI of OBP-301 plus 10 MOI of Ad/Bax, and harvested at day 4; cell cycle analysis using flow cytometry was then performed. The histograms were analyzed with FlowJO software.

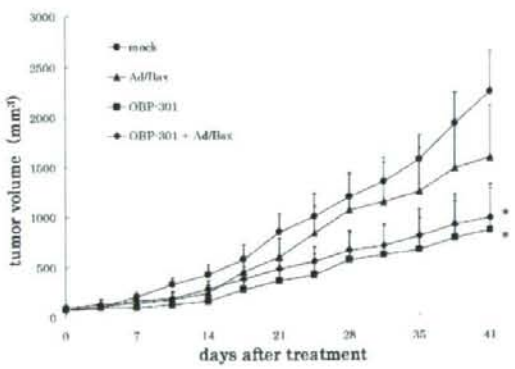

FIGURE 4 – Tumor xenograft size after infection with OBP-301, Ad/Bax, or their combination. A549 xenografts were established in nude mice (Balb/c nu/nu) through subcutaneous inoculation of 2×10^6 A549 cells into the dorsal flank. When the tumor reached a diameter of ~5 mm, the virus solution was injected into the tumor at a dose of 1×10^7 PFU/body on 3 consecutive days. Tumor volume was calculated using the equation $a \times b^2 \times 0.5$, in which a and b are the largest and smallest diameters, respectively. Bars, standard error (SE). *, $p < 0.05$, compared with mock-treated tumors.

flank of nude mice and the virus was injected into the tumor at a dose of 1×10^7 PFU/body on 3 consecutive days. Tumor size was measured 2–3 times a week and followed for up to 41 days. Treatment with Ad/Bax alone did not suppressed tumor growth significantly when compared with mock treatment because of a suboptimal dose, whereas treatments with OBP-301 and OBP-301 plus Ad/Bax significantly suppressed tumor growth when compared with other controls ($p \leq 0.05$; Fig. 4). However, the effect of adding Ad/Bax to OBP-301 treatment was less than expected, and the difference was not significant.

We also examined the antitumor effects of this combination treatment in mice with pleurally disseminated A549 tumors. The mice were injected with 100 μl of 1.0×10^7 PFU of OBP-301, Ad/Bax, or both into the thoracic space on 3 consecutive days. Three weeks after cell inoculation, the mice were killed and their thoracic spaces were examined macroscopically for any growths. To quantitate the reduction of tumor burden in the thoracic spaces, the tumors were removed and weighed. Although treatment with OBP-301 alone or Ad/Bax in combination with OBP-301 significantly suppressed tumor weight, there was no significant difference between them (Figs. 5*a* and 5*b*). These results suggest that Bax gene therapy does not augment oncolytic virotherapy *in vivo*.

Combination treatment resulted in suppressed E1A protein expression due to reduced viral replication in vitro

To explore the underlying mechanism by which oncolytic virotherapy did not work cooperatively with proapoptotic Bax gene therapy, E1A protein expression was examined by Western blot analysis. A549 cells were treated with each virus singly or in combination and then subjected to the analysis at days 3 and 5. Treatment with OBP-301 alone and in combination treatment with Ad/lacZ demonstrated increased E1A protein expression, meaning efficient viral replication. Treatment with Ad/Bax alone showed no E1A protein expression because of the E1-deficient replication incompetent virus. Of note, treatment with OBP-301 plus Ad/Bax showed suppressed expression of E1A protein when compared with treatment with OBP-301 alone, meaning that the combination with Ad/Bax may interfere with viral replication (Fig. 6).

To further document the effect of Bax expression on the process of viral propagation, the replication and release of viral progenies were measured by quantitative real time PCR. A549 cells were infected with viruses and the supernatants of the cell groups were collected. DNA was extracted from them and subjected to the assay. We found suppressed viral copy numbers in cells treated with the combinations with Ad/Bax and Ad/lacZ (Fig. 7). The inhibition of E1A copy numbers in a group of Ad/Bax combination was about 10 times of inhibition in a group of Ad/lacZ combination. Our results suggest that Bax gene therapy may interfere with viral production and thus be not conducive to oncolytic virotherapy. To further examine viral replication *in vivo*, the amounts of infectious viruses produced in the tumors were analyzed. Titers were very low for tumors treated with Ad/Bax because of a lack of replication in the absence of E1 gene, while tumors treated with OBP-301 produced higher amount of infectious virus than those treated with Ad/Bax alone, suggesting viral replication in tumors. However, because of the large variation in data from each group, there was no significant difference between treatment groups (data not shown).

Discussion

Replication-competent oncolytic adenovirus has shown a remarkable safety profile but efficacy for cancer therapy continues to be a major obstacle. To eliminate cancer cells, the virus also must spread throughout the bulk of the tumor and induce cell

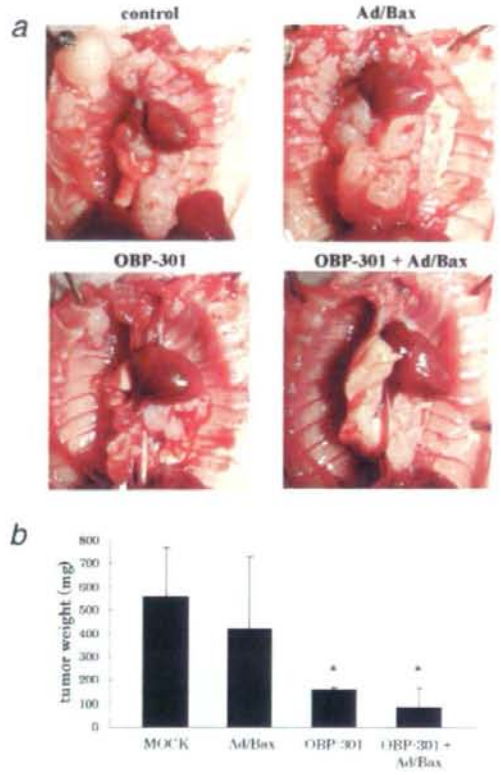

FIGURE 5 – Antitumor effects of OBP-301 combined with Ad/Bax in mice with A549 pleural dissemination. Mice were inoculated with 2×10^6 A549 cells into the pleural cavity, and 24 hr after tumor injection, 100 μl of 1.0×10^7 PFU of OBP-301, Ad/Bax, both of them, or PBS was injected into the thoracic space. The procedure was repeated over 3 consecutive days. (*a*) Three weeks after cell inoculation, mice were killed and their thoracic spaces were examined macroscopically for any growths. (*b*) Tumors in the thoracic spaces were removed and weighed. Bars, SD. *, $p < 0.05$, compared with mock-treated tumors.

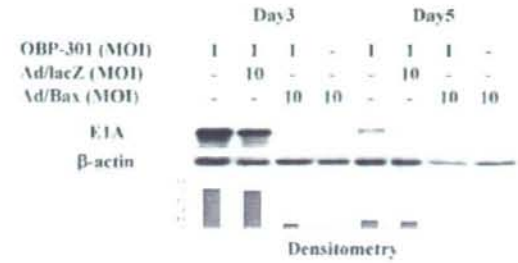

FIGURE 6 – Expression of E1A in cells infected with Ad/Bax in combination with OBP-301. A549 cells were infected at 1 MOI of OBP-301 alone, 10 MOI of Ad/Bax alone, or 1 MOI of OBP-301 in combination with 10 MOI of Ad/Bax or Ad/lacZ, and then harvested at day 3 or 5. Lysates were subjected to immunoblot analysis with antibodies recognizing E1A or β-actin. The lower panel shows the intensity of each band of Bax determined by densitometric scanning using NIH image software and normalized by dividing the actin signal.

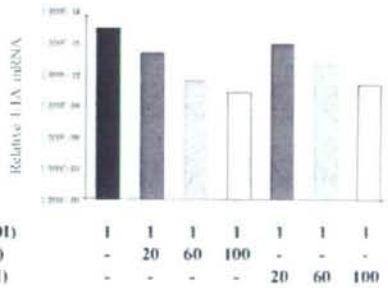

FIGURE 7 – Assessment of viral DNA replication in cells infected with Ad/Bax in combination with OBP-301. A549 cells were seeded on 25-cm^2 flasks at 5×10^5 cells 15 hr before infection. Cells were infected with OBP-301 alone, Ad/Bax alone, or their combination at an MOI of 1 PFU/cell 15 hr later. The cells were harvested at 48 hr and then subjected to real-time quantitative PCR assay. The amounts of viral E1A copy number are defined as the fold increase for each sample relative to that at 2 hr (2 hr equals 1).

death. Even with replicating adenoviral systems, the necessity to infect all cancer cells remains a major challenge.

In this study, we hypothesized that the oncolytic adenovirotherapy combined with Bax gene therapy could enhance the oncolytic potency. As expected, the combination treatment resulted in Bax overexpression, induced early apoptosis and enhanced efficacy in the cell viability assay *in vitro*. However, disappointingly, combination treatment did not result in further reductions in flank tumor size and pleural disseminated tumor weight, which was associated with suppressed E1A protein expression and reduced viral replication of OBP-301.

The antitumor effect of the oncolytic virus depends on the cytopathic effect intrinsic to adenovirus replication and dissemination throughout the tumor mass. Because viral infection of the tumor bulk depends on cell-to-cell viral spread, there may be a race between rapid tumor growth and viral spread. Therefore, to improve the efficacy of oncolytic virotherapy, the accelerated viral release and induction of cell death must be necessary. A previous study has shown that loss of E1b-19kD function in a replicating adenovirus enhances early viral release, leading to accelerated cell-to-cell viral spread.[17] In turn, Chiou and White reported that inhibition of apoptosis could severely attenuate viral release.[18] Taken together, this suggests that a combination of proapoptotic gene therapy and oncolytic virotherapy may improve the antitumor efficacy by enhancing cell-to-cell spread of the virus. The other rationale of the combination of proapoptotic gene therapy is to cope with the cancer resistance to the oncolytic virotherapy. Because heterogeneity in cancer cell populations drives the development of resistance, the approach of killing cells by multiple nonoverlapping mechanisms could be a solution. Although an oncolytic virus can kill cells by apoptosis-independent mechanisms such as direct cell lysis and necrosis, cells treated with combination therapy showed a pattern of apoptosis evidenced by analysis of the cell cycle. However, because induction of apoptosis and premature cell lysis may potentially compromise viral yield, reduced viral production could be a concern in using Bax-expressing virus in combination.

In the *in vitro* cell viability assay, the combination of Bax-expressing adenovirus with a replicating adenovirus leads to increased apoptosis at an earlier phase as theoretically anticipated. In turn, we have demonstrated a reduced viral yield in A549 cells. The early apoptotic cell death induced by Bax overexpression may limit an increase of virus and disturb viral replication. Our results are consistent with those of Lambright *et al.*,[19] who found that the addition of ganciclovir therapy to a replicating vector containing the HSVtk suicide gene did not augment efficacy, despite the enhanced production of the transgene. Viral replication and timely cell-death induction thus need to be well coordinated, and forced

induction of early apoptosis could be a cause of losing the combinative effect. Our data suggest that impaired viral replication may offset the benefits due to enhanced transgene spread *in vivo*.

In this study, we have shown the discrepancy between *in vitro* and *in vivo* findings, but this would not result solely from the reduced viral replication. Although viruses can rapidly and evenly spread in cell culture monolayer, this would not be expected in a solid tumor. In a tumor mass, it is very difficult to distribute viral progenies to even the majority of tumor cells. Because a cancer-targeting oncolytic virus is designed to selectively replicate in cancer cells, the normal interstitial cells would be obstacles. The virus would also face other obstacles for viral distribution, including tight intercellular space and continuous drainage by the circulatory and lymphatic systems. In this circumstance, the intratumoral dispersion is confined to one part of the tumor, and thus the requirement of double infection in a complementary strategy curtails the efficacy at low multiplicities of infection.

Although our data suggest that Bax gene therapy in combination with oncolytic adenovirotherapy is not likely to be therapeutically beneficial, the concept of "armed" replicating adenovirotherapy still has potential merit. Overexpression of the adenoviral death protein, expression of TRAIL and deletion of the E1B-19kD gene have all been shown to improve viral spread and efficacy of replicating adenoviruses *in vitro* and *in vivo*.[5,17,20–25] Various suicide genes or cytokines have also been expressed with replication-competent vectors to improve cell killing.[26–30] One important factor to keep in mind is to enhance antitumor effect without inhibiting the proliferative capacity of viruses.

In summary, oncolytic adenovirotherapy in combination with Bax gene therapy resulted in augmented cell killing *in vitro*. However, in a xenografted tumor model, oncolytic efficacy was not improved; this was associated with suppressed E1A protein expression and reduced viral replication. Bax gene therapy may possibly interfere with viral production and thus be not conducive to oncolytic virotherapy.

Acknowledgements

This work was supported in part by grants from the Ministry of Education, Culture, Sports, Science and Technology of Japan (T.F. and S.K.); and by grants from the Ministry of Health, Labour and Welfare of Japan (T.F. and S.K.).

References

1. Hawkins LK, Lemoine NR, Kirn D. Oncolytic biotherapy: a novel therapeutic platform. Lancet Oncol 2002;3:17–26.
2. Chiocca EA. Oncolytic viruses. Nat Rev Cancer 2002;2:938–50.
3. Nemunaitis J, Khuri F, Ganly I, Arseneau J, Posner M, Vokes EK, McCarty T, Landers S, Blackburn A, Romel L, Randlev B, Kaye S, et al. Phase II trial of intratumoral administration of ONYX-015, a replication-selective adenovirus, in patients with refractory head and neck cancer. J Clin Oncol 2001;19:289–98.
4. Khuri FR, Nemunaitis J, Ganly I, Arseneau J, Tannock IF, Romel L, Gore M, Ironside J, MacDougall RH, Heise C, Randlev B, Gillenwater AM, et al. A controlled trial of intratumoral ONYX-015, a selectively-replicating adenovirus, in combination with cisplatin and 5-fluorouracil in patients with recurrent head and neck cancer. Nat Med 2000;6:879–85.
5. Harrison D, Sauthoff H, Heitner S, Jagirdar J, Rom W, Hay J. Wild-type adenovirus decreases tumor xenograft growth, but despite viral persistence complete tumor responses are rarely achieved-deletion of the viral E1b-19kDa gene increases the oncolytic effect. Hum Gene Ther 2001;12:1323–32.
6. DeWeese TL, van der Poel H, Li S, Mikhak B, Drew R, Goemann M, Hamper U, DeJong R, Detorie N, Rodriguez R, Haulk T, DeMarzo AM, et al. A phase I trial of CV706, a replication-competent, PSA selective oncolytic adenovirus, for the treatment of locally recurrent prostate cancer following radiation therapy. Cancer Res 2001;61:7464–72.
7. Reid T, Galanis E, Abbruzzese J, Sze D, Wein LM, Andrews J, Randlev B, Heise C, Uprichard M, Hatfield M, Rome L, Rubin J, et al. Hepatic arterial infusion of a replication-selective oncolytic adenovirus (dl1520): phase II viral, immunologic, and clinical endpoints. Cancer Res 2002;62:6070–79.
8. Hamid O, Varterasian ML, Wadler S, Hecht JR, Benson A, Galanis E, Uprichard M, Omer C, Bycott P, Hackman RC, Shields AF. Phase II trial of intravenous CI-1042 in patients with metastatic colorectal cancer. J Clin Oncol 2003;21:1498–504.
9. Jurgensmeier JM, Xie Z, Deveraux Q, Ellerby L, Bredesen D, Reed JC. Bax directly induces release of cytochrome c from isolated mitochondria. Proc Natl Acad Sci USA 1998;95:4997–5002.
10. Pastorino JG, Chen ST, Tafani M, Snyder JW, Farber JL. The overexpression of Bax produces cell death upon induction of the mitochondrial permeability transition. J Biol Chem 1998;273:7770–5.
11. Kagawa S, Pearson SA, Ji L, Xu K, McDonnell TJ, Swisher SG, Roth JA, Fang B. A binary adenoviral vector for expressing high levels of the proapoptotic gene bax. Gene Ther 2000;7:75–9.
12. Kagawa S, Gu J, Swisher SG, Ji L, Roth JA, Lai D, Stephens LC, Fang B. Antitumor effect of adenovirus-mediated Bax gene transfer on p53-sensitive and p53-resistant cancer lines. Cancer Res 2000;60:1157–61.
13. Tsunemitsu Y, Kagawa S, Tokunaga N, Otani S, Umeoka T, Roth JA, Fang B, Tanaka N, Fujiwara T. Molecular therapy for peritoneal dissemination of xenotransplanted human MKN-45 gastric cancer cells with adenovirus mediated Bax gene transfer. Gut 2004;53:554–60.
14. Kawashima T, Kagawa S, Kobayashi N, Shirakiya Y, Umeoka T, Teraishi F, Taki M, Kyo S, Tanaka N, Fujiwara T. Telomerase-specific replication-selective virotherapy for human cancer. Clin Cancer Res 2004;10:285–92.
15. Maizel JV, Jr, White DO, Scharff MD. The polypeptides of adenovirus. I. Evidence for multiple protein components in the virion and a comparison of types 2, 7A, and 12. Virology 1968;36:115–25.
16. Kanegae Y, Makimura M, Saito I. A simple and efficient method for purification of infectious recombinant adenovirus. Jpn J Med Sci Biol 1994;47:157–66.
17. Sauthoff H, Heitner S, Rom WN, Hay JG. Deletion of the adenoviral E1b-19kD gene enhances tumor cell killing of a replicating adenoviral vector. Hum Gene Ther 2000;11:379–88.
18. Chiou SK, White E. Inhibition of ICE-like proteases inhibits apoptosis and increases virus production during adenovirus infection. Virology 1998;244:108–18.
19. Lambright ES, Amin K, Wiewrodt R, Force SD, Lanuti M, Propert KJ, Litzky L, Kaiser LR, Albelda SM. Inclusion of the herpes simplex thymidine kinase gene in a replicating adenovirus does not augment antitumor efficacy. Gene Ther 2001;8:946–53.
20. Liu TC, Hallden G, Wang Y, Brooks G, Francis J, Lemoine N, Kirn D. An E1B-19kDa gene deletion mutant adenovirus demonstrates tumor necrosis factor-enhanced cancer selectivity and enhanced oncolytic potency. Mol Ther 2004;9:786–803.
21. Kim J, Cho JY, Kim JH, Jung KC, Yun CO. Evaluation of E1B gene-attenuated replicating adenoviruses for cancer gene therapy. Cancer Gene Ther 2002;9:725–36.
22. Doronin K, Toth K, Kuppuswamy M, Ward P, Tollefson AE, Wold WS. Tumor-specific, replication-competent adenovirus vectors overexpressing the adenovirus death protein. J Virol 2000;74:6147–55.
23. Sova P, Ren XW, Ni S, Bernt KM, Mi J, Kiviat N, Lieber A. A tumor-targeted and conditionally replicating oncolytic adenovirus vector expressing TRAIL for treatment of liver metastases. Mol Ther 2004;9:496–509.
24. Liu XY, Qiu SB, Zou WG, Pei ZF, Gu JF, Luo CX, Ruan HM, Chen Y, Qi YP, Qian C. Effective gene—virotherapy for complete eradication of tumor mediated by the combination of hTRAIL (TNFSF10) and plasminogen k5. Mol Ther 2005;11:531–41.
25. Ye X, Lu Q, Zhao Y, Ren Z, Ren XW, Qiu QH, Tong Y, Liang M, Hu F, Chen HZ. Conditionally replicative adenovirus vector carrying TRAIL gene for enhanced oncolysis of human hepatocellular carcinoma. Int J Mol Med 2005;16:1179–84.
26. Bristol JA, Zhu M, Ji H, Mina M, Xie Y, Clarke L, Forry-Schaudies S, Ennist DL. In vitro and in vivo activities of an oncolytic adenoviral vector designed to express GM-CSF. Mol Ther 2003;7:755–64.
27. Ramesh N, Ge Y, Ennist DL, Zhu M, Mina M, Ganesh S, Reddy PS, Yu DC. CG0070, a conditionally replicating granulocyte macrophage colony-stimulating factor—armed oncolytic adenovirus for the treatment of bladder cancer. Clin Cancer Res 2006;12:305–13.
28. Zhao L, Gu J, Dong A, Zhang Y, Zhong L, He L, Wang Y, Zhang J, Zhang Z, Huiwang J, Qian Q, Qian C, et al. Potent antitumor activity of oncolytic adenovirus expressing mda-7/IL-24 for colorectal cancer. Hum Gene Ther 2005;16:845–58.
29. Nanda D, Vogels R Havenga M, Avezaat CJ, Bout A, Smitt PS. Treatment of malignant gliomas with a replicating adenoviral vector expressing herpes simplex virus-thymidine kinase. Cancer Res 2001;61:8743–50.
30. Lee CT, Park KH, Yanagisawa K, Adachi Y, Ohm JE, Nadaf S, Dikov MM, Curiel DT, Carbone DP. Combination therapy with conditionally replicating adenovirus and replication defective adenovirus. Cancer Res 2004;64:6660–5.

Gene Therapy (2008) 15, 1233–1239

www.nature.com/gt

SHORT COMMUNICATION

Autophagy-inducing agents augment the antitumor effect of telomerase-selective oncolytic adenovirus OBP-405 on glioblastoma cells

T Yokoyama[1,8], E Iwado[1,8], Y Kondo[1], H Aoki[1], Y Hayashi[2], MM Georgescu[2], R Sawaya[1,3], KR Hess[4], GB Mills[5], H Kawamura[6], Y Hashimoto[6], Y Urata[6], T Fujiwara[6,7] and S Kondo[1,3]

[1]Department of Neurosurgery, The University of Texas MD Anderson Cancer Center, Houston, TX, USA; [2]Department of Neuro–Oncology, The University of Texas MD Anderson Cancer Center, Houston, TX, USA; [3]Department of Neurosurgery, Baylor College of Medicine, Houston, TX, USA; [4]Department of Biostatistics and Applied Mathematics, The University of Texas MD Anderson Cancer Center, Houston, TX, USA; [5]Department of Molecular Therapeutics, The University of Texas MD Anderson Cancer Center, Houston, TX, USA; [6]Oncolys BioPharma Inc., Tokyo, Japan and [7]Division of Surgical Oncology, Department of Surgery, Okayama University Graduate School of Medicine and Dentistry, Okayama, Japan

Oncolytic adenoviruses are a promising tool in cancer therapy. In this study, we characterized the role of autophagy in oncolytic adenovirus-induced therapeutic effects. OBP-405, an oncolytic adenovirus regulated by the human telomerase reverse transcriptase promoter (hTERT-Ad, OBP-301) with a tropism modification (RGD) exhibited a strong antitumor effect on glioblastoma cells. When autophagy was inhibited pharmacologically, the cytotoxicity of OBP-405 was attenuated. In addition, autophagy-deficient Atg5$^{-/-}$ *mouse embryonic fibroblasts (MEFs) were less sensitive than wild-type MEFs to OBP-405. These findings indicate that OBP-405-induced autophagy is a cell killing effect. Moreover, autophagy-inducing therapies (temozolomide and rapamycin) synergistically sensitized tumor cells to OBP-405 by stimulating the autophagic pathway without altering OBP-405 replication. Mice harboring intracranial tumors treated with OBP-405 and temozolomide survived significantly longer than those treated with temozolomide alone, and mice treated with OBP-405 and the rapamycin analog RAD001 survived significantly longer than those treated with RAD001 alone. The observation that autophagy inducers increase OBP-405 antitumor activity suggests a novel strategy for treating patients with glioblastoma.*
Gene Therapy (2008) **15**, 1233–1239; doi:10.1038/gt.2008.98; published online 26 June 2008

Keywords: *autophagy; glioblastoma; OBP-301; OBP-405*

Oncolytic adenoviruses have recently been developed as a novel cancer therapy.[1,2] We have shown that the oncolytic adenovirus regulated by the human telomerase reverse transcriptase promoter (hTERT-Ad) induces nonapoptotic autophagy in glioblastoma cells.[3] However, the molecular machinery underlying autophagy-induced cell death remains unclear.[4–6] Furthermore, the processes determining whether autophagy in cancer cells causes death or acts as a protective mechanism activated during cellular distress are unknown. In this study, we elucidated the therapeutic role of autophagy in hTERT-Ad infection.

The infection efficiency of adenoviral constructs, which are derived from human adenovirus serotype 5, varies widely depending on the cellular expression of the coxsackievirus and adenovirus receptor (CAR).[7] Modification of the adenoviral fiber protein is one approach to overcoming the limitation imposed by this dependence on CAR.[8] A recent study demonstrated the activity of OBP-405, which is an hTERT-Ad with a tropism modification (RGD): OBP-405 had a profound oncolytic effect *in vitro* and *in vivo* on lung and colon cancer cells regardless of the CAR expression level.[9] In addition, for cells with low CAR expression levels, OBP-405 had a higher rate of infection than did OBP-301, an hTERT-Ad that expresses the *E1A* gene under the control of a 455-bp hTERT promoter.[9] The hTERT-Ad that we used previously has a 255-bp hTERT promoter.[3]

Good manufacturing practice OBP-301 (Telomelysin) and OBP-405 (Telomelysin-RGD) were used in the current study. We first determined the expression levels of CAR and integrins (αvβ3 and αvβ5) on the cell surface of glioblastoma cells. To predict the response of human glioblastoma to OBP-301 or OBP-405, the established cell lines U87-MG, U251-MG, D54, and U373-MG and primary MDC-01 cells isolated from glioblastoma tissue were used. The U87-MG, D54 and MDC-01 cells expressed the lowest levels of CAR, whereas the U251-MG cells expressed the highest level of CAR (Figure 1a). In contrast, αvβ3 and αvβ5 integrins were highly expressed in each of these glioblastoma cells. Cells that expressed low levels of CAR were resistant to OBP-301 infection, whereas OBP-405 effectively decreased viabi-

Correspondence: Dr T Yokoyama, Department of Neurosurgery, The University of Texas MD Anderson Cancer Center, Unit BSRB 1004, 1515 Holcombe Blvd., Houston, TX 77030, USA.
E-mail: tyokoyama@mdanderson.org
[8]These authors contributed equally to this work.
Received 26 January 2008; revised 1 April 2008; accepted 1 April 2008; published online 26 June 2008

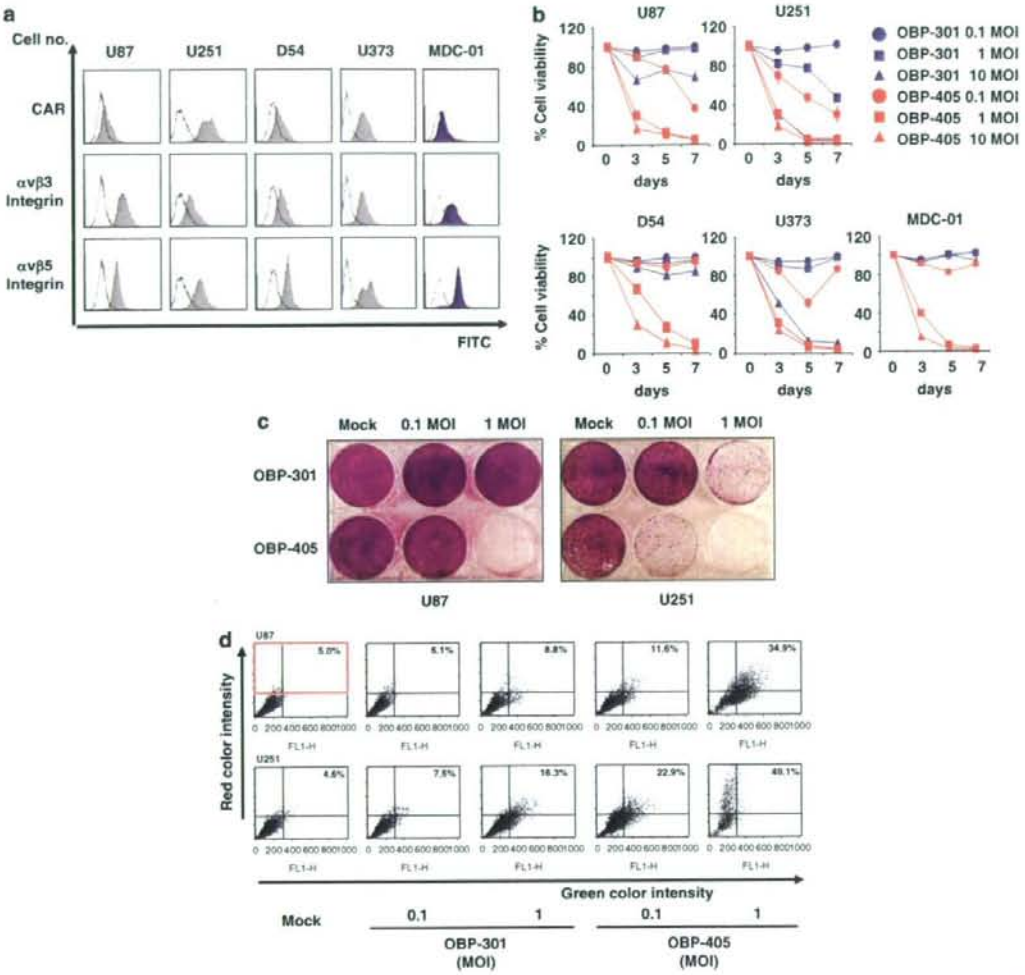

Figure 1 (**a**) Flow cytometric analysis of CAR and integrin (αvβ3 and αvβ5) expression on glioblastoma cells. Human glioblastoma cell lines U87-MG, U251-MG, D54 and U373-MG were purchased from American Type Culture Collection (Manassas, VA, USA). Primary glioblastoma MDC-01 cells were isolated from surgical specimens of glioblastoma at MD Anderson Cancer Center and were positive for telomerase and glial-fibrillary acidic protein. Cells were incubated with anti-CAR (Upstate Biotechnology, Lake Placid, NY, USA), anti-αvβ3 integrin and anti-á,β5 integrin (Chemicon International, Temecula, CA, USA) monoclonal antibodies and then detected with fluorescein isothiocyanate (FITC)-labeled rabbit anti-mouse IgG secondary antibody (Zymed Laboratories, San Francisco, CA, USA). Open areas (control), isotype-matched normal mouse IgG1 conjugated to FITC. (**b**) Effect of OBP-301 and OBP-405 on the viability of glioblastoma cells. Cells were infected at the indicated MOI values and surviving cells were quantified over 7 days by the use of WST-1 assay (Roche Applied Science, Indianapolis, IN, USA). Results shown are the means ± s.d. of three independent experiments. (**c**) Oncolytic effect of OBP-301 and OBP-405 on glioblastoma cells. Low-CAR expressing (U87-MG) and high-CAR expressing (U251-MG) cells were stained with 0.5% crystal violet (Sigma-Aldrich, St Louis, MO, USA) 5 days after infection. (**d**) Development of acidic vesicular organelles (AVOs) in U87-MG and U251-MG cells infected with OBP-301 or OBP-405 at an MOI of 0.1 or 1.0 for 72 h. Mock- or virus-infected cells were stained with 1.0 μg ml^{-1} acridine orange (Polysciences, Warrington, PA, USA) for 15 min at room temperature and analyzed using a flow cytometer (FACScan; Becton Dickinson, San Jose, CA, USA). In acridine orange-stained cells, the cytoplasm and nucleus fluorescence bright green and dim red, whereas acidic compartments fluorescence bright red.[10,11] The intensity of the red fluorescence is proportional to the degree of acidity and volume of AVOs. Top of grid was considered as AVOs. CAR, coxsackievirus and adenovirus receptor; IgG, immunoglobulin G; MOI, multiplicity of infection.

lity of glioblastoma cells (Figure 1b). In addition, OBP-405 killed the cells more efficiently than did OBP-301, and neither OBP-301 nor OBP-405 induced apoptosis (Figure 1c) (Supplementary Figures 1a–c).

Nonapoptotic autophagy is characterized by the development of acidic vesicular organelles (AVOs).[10] Compared with mock infection, both OBP-301 and OBP-405 increased the percentage of AVO-positive cells in a multiplicity of infection (MOI)-dependent manner (Figure 1d). As expected, OBP-405 induced the development of AVOs more efficiently than did OBP-301.

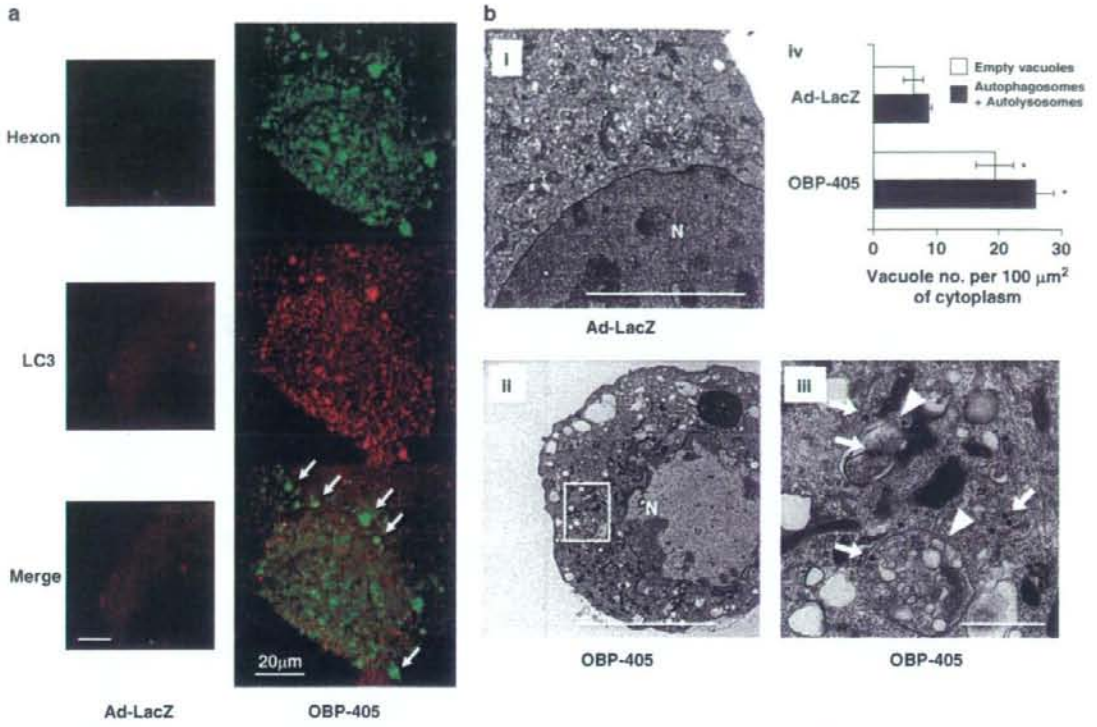

Figure 2 (**a**) Localization of the adenoviral protein hexon and autophagic LC3B protein in glioblastoma cells infected with Ad-LacZ or OBP-405 at an MOI of 0.5. After infection for 72 h, U87-MG cells were processed for fluorescent immunocytostaining with anti-LC3B (1:5000 dilution) and antiadenovirus 1, 2, 5 and 6 hexon (Chemicon International) antibodies. Anti-LC3B antibody was generated as described previously.[14,15] The slides were monitored using inverted microscope (ECRIPSE TE2000-U; Nikon, Melville, NY, USA) and the data were deconvolved and analyzed using AutoQuant's AutoDeBlur software (MediaCybernetics, Bethesda, MD, USA). The arrow shows the colocalization of LC3B and hexon. (**b**) Electron photomicrographs showing the ultrastructure, including the nucleus (N) of glioblastoma cells treated with nonreplicating adenovirus carrying the Ad-LacZ or OBP-405 at an MOI of 0.5 for 72 h. (**i**) Ad-LacZ-infected U87-MG cells; few autophagic vacuoles were observed, scale bar = 10 μm. (**ii**) OBP-405-infected U87-MG cells, scale bar = 10 μm. (**iii**) A magnified view of the area boxed in (ii), scale bar = 1 μm. The arrow indicates viral particles and the arrowhead indicates an autophagosome that includes residual material and virus particles in the cytoplasm. (**iv**) Autophagosomes and autolysosomes were quantified, as described previously.[16,17] $^{*}P < 0.05$ vs Ad-LacZ. MOI, multiplicity of infection.

The green fluorescent protein (GFP)-tagged expression vector of LC3 is a useful tool with which to detect autophagy.[12] On fluorescence microscopy, GFP-LC3-transfected U87-MG cells showed the diffuse distribution of GFP-LC3 with mock infection, whereas infection with OBP-405 at an MOI of 1.0 resulted in a punctate pattern of GFP–LC3 (Supplementary Figure 2a). This pattern represents autophagic vacuoles and indicated that OBP-405 induced autophagy. With both OBP-301 and OBP-405, the percentage of GFP–LC3 dots increased in an MOI-dependent manner; this increase was considerably higher with OBP-405 than with OBP-301.

The LC3 protein exists in two cellular forms, LC3-I and LC3-II. LC3-I is converted to LC3-II by conjugation to phosphatidylethanolamine, and the amount of LC3-II is closely correlated with the number of autophagosomes.[13] In both U87-MG and U251-MG cells, the amount of LC3-II was increased by infection with OBP-301 or OBP-405 in an MOI-dependent manner and by OBP-405 in a time-dependent manner (Supplementary Figure 2b). These results indicated that OBP-405 caused more autophagy in glioblastoma cells than OBP-301 did.

To analyze the association between adenoviral infection and autophagy, we determined the localization of OBP-405 and autophagic vacuoles. The adenoviral hexon was detected in the cytoplasm 6 h after infection, but at that point, autophagic vacuoles positive for the isoform B of human LC3 (LC3B) were not observed (Supplementary Figure 3), indicating that autophagy was not initiated. Twenty-four hours after infection, hexon was detected in the cytoplasm and nucleus and LC3B-positive autophagic vacuoles were observed. At 48 h, the cell and nucleus had become larger. At 72 h after infection, the majority of the autophagic vacuoles were colocalized with hexon-positive adenoviruses (Figure 2a). In addition, we analyzed the ultrastructure of infected U87-MG cells. U87-MG cells infected with control nonreplicating adenovirus (Ad-LacZ) exhibited few autophagic features, whereas autophagic vacuoles, autolysosomes and empty vacuoles were observed after infection with OBP-405. Most OBP-405-infected cells

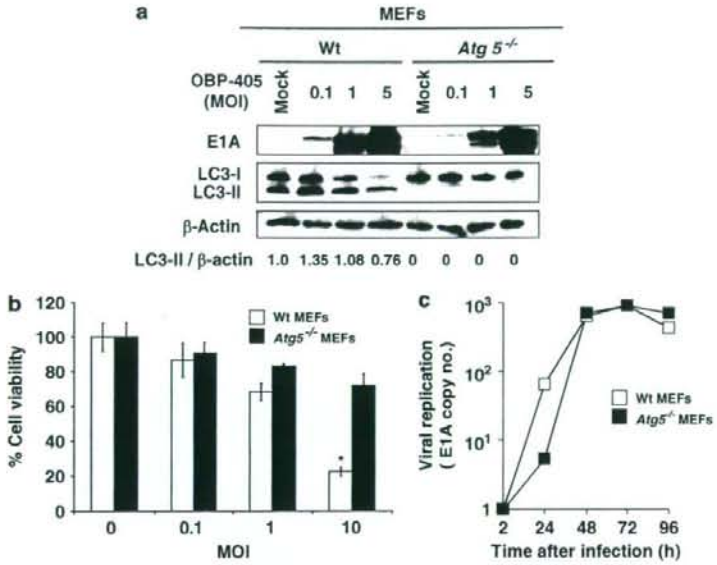

Figure 3 (a) Effect of OBP-405 infection on the wild-type and *Atg5*$^{-/-}$ MEFs (kindly provided by Dr N Mizushima). The expression of E1A (BD Biosciences Pharmingen, San Diego, CA, USA) and an amount of LC3-II in MEFs infected with OBP-405 at an MOI of 0–5.0 for 72 h was assessed by western blotting. The intensities of the amount of LC3-II bands were normalized by the bands' intensities of β-actin (Sigma-Aldrich), using Bio-Rad Fluor-S Multiimager (Bio-Rad Laboratories, Hercules, CA, USA). (b) Effect of OBP-405 on the viability of wild-type and *Atg5*$^{-/-}$ MEFs. MEFs were infected with OBP-405 at an MOI of 0 to 10 for 48 h, and cell viability was assessed by WST-1 assay. *$P<0.01$ vs *Atg5*$^{-/-}$ MEFs. (c) E1A viral replication of wild-type and *Atg5*$^{-/-}$ MEFs infected with OBP-405 at an MOI of 1.0. The cells were incubated at 37 °C for the indicated periods, trypsinized and harvested for intracellular replication analysis at 2, 24, 48, 72 and 96 h. DNA purification was performed with the QIAmp DNA mini kit (Qiagen, Valencia, CA, USA). The E1A DNA copy number was determined by quantitative real-time PCR, using a Power SYBR Green PCR Master Mix (Applied Biosystems, Foster, CA, USA) and 7500 real-time PCR systems (Applied Biosystems), as described previously.[9] The amount of viral E1A copy number is defined as the fold increase for each sample relative to that at 2 h. MEFs, mouse embryonic fibroblasts; MOI, multiplicity of infection

exhibited viral particles in the nucleus and cytoplasm, but they exhibited neither the chromatin condensation nor the DNA fragmentation that is the characteristic of apoptosis (Figure 2b). Interestingly, viral particles were observed inside autophagic vacuoles. These results suggested that OBP-405 infection initiated the autophagic process and that the autophagic vacuoles sequestered replicating OBP-405.

To assess the role of autophagy in OBP-405 infection, we inhibited the OBP-405-induced autophagy pharmacologically by using 3-methyladenine (3-MA);[18] the decreased viability of these cells was significantly reversed ($P<0.01$) (Supplementary Figures 4a and b). However, the inhibition of autophagy did not affect the increase in E1A copy number of OBP-405 (Supplementary Figure 4c). To exclude the possibility that the effects of 3-MA are independent of inhibition of autophagy, we inhibited autophagy specifically by using small interfering RNA (siRNA) directed against *autophagy-related gene 5* (*Atg5*), which is essential for autophagosome formation. Transfection with *Atg5* siRNA effectively inhibited OBP-405-induced autophagy and recovered the OBP-405-inhibited viability of U87-MG and U251-MG cells (Supplementary Figure 5a–c). Together, the results indicated that OBP-405 induced cell death through autophagy.

In addition, *Atg5*$^{-/-}$ mouse embryonic fibroblasts (MEFs) were significantly more resistant to OBP-405-induced death than the wild-type MEFs ($P<0.01$) (Figures 3a and b). This observation supported our results with 3-MA and *Atg5* siRNA. Similar to 3-MA, viral replication of OBP-405 did not differ significantly between the wild-type and *Atg5*$^{-/-}$ MEFs (Figure 3c).

The above observations prompted us to hypothesize that the antitumor effect of OBP-405 would be augmented by the combinatorial therapy with other autophagy-inducing agents. To test our hypothesis, we combined OBP-405 with rapamycin, an inhibitor of the mammalian target of rapamycin and the DNA-alkylating agent temozolomide (TMZ), both of which efficiently induce autophagy.[19,20] Rapamycin and TMZ not only enhanced OBP-405-induced autophagy *in vitro* but also synergized with OBP-405 to induce the death of glioblastoma cells (Figures 4a and b; Supplementary Figure 6). In contrast, TMZ or rapamycin did not alter viral replication (Figure 4c). Thus OBP-405 synergizes with autophagy-inducing agents to increase cell death *in vitro*.

To determine whether the *in vitro* effect of OBP-405 with TMZ or rapamycin translates to greater activity *in vivo*, we established intracranial tumors in nude mice. Compared with mice treated with Ad-LacZ, mice treated with OBP-405 lived significantly longer (mean survival = 27.5 vs 34.0 days; difference (95% confidence interval) = 6.0 (3.0–9.1) days; $P=0.0008$) (Figure 5a). Mice treated with TMZ also survived significantly longer (mean survival = 27.5 vs 37.0 days; difference = 10

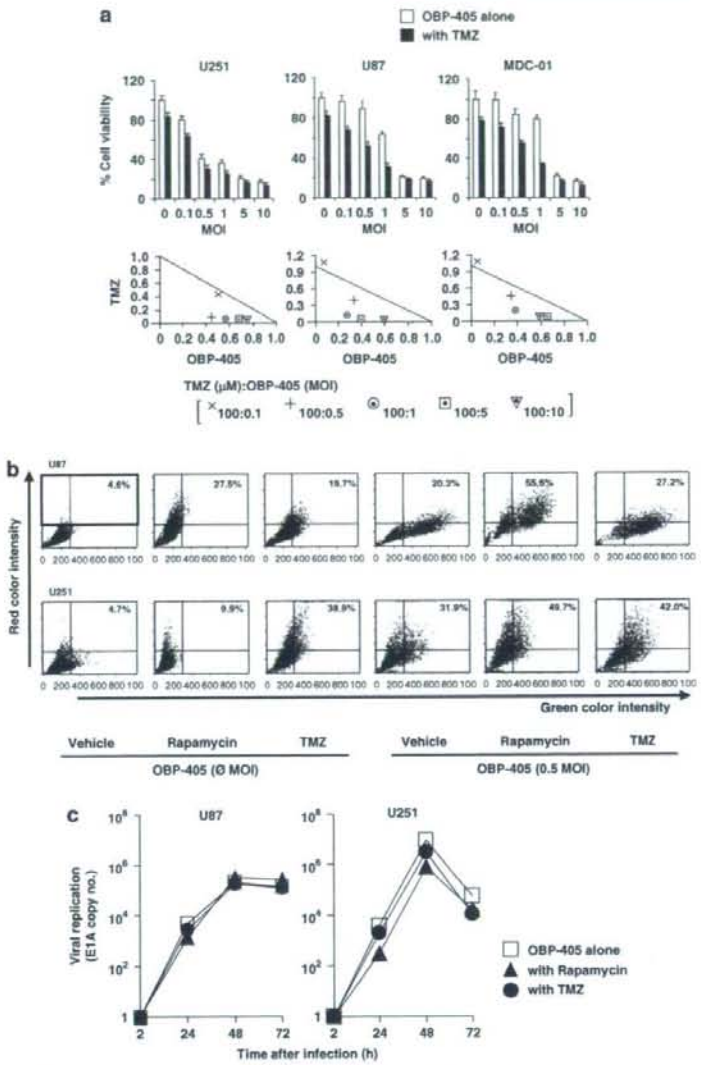

Figure 4 (a) Combined effects of OBP-405 with TMZ on glioblastoma cells. U251-MG, U87-MG and MDC-01 cells were infected with OBP-405 at an MOI of 0 to 10 in the presence of 100 μM TMZ (purchased from a pharmacy in The University of Texas MD Anderson Cancer Center) for 72 h for the WST-1 assay. The combined effect of OBP-405 with TMZ was analyzed with the combination index (CI)-isobologram using CalcuSyn software (Biosoft, Ferguson, MO, USA), as described previously.[19] In the isobologram, a plot on the diagonal line indicates that the combination is simply additive. A plot to the left under the line indicates that the combination is synergistic, whereas a plot to the right above the line indicates that it is antagonistic. Each plot represents values generated in at least three independent experiments for the simultaneous treatment of cells. (b) Development of acidic vesicular organelles (AVOs) in U87-MG and U251-MG cells infected with OBP-405 at an MOI of 0.5 in the presence of 1 nM rapamycin (Sigma-Aldrich) or 100 μM TMZ were stained with 1.0 μg ml^{-1} acridine orange as described previously.[10,11] Top of grid was considered as AVOs. (c) E1A viral replication of U87-MG and U251-MG cells infected with OBP-405 at an MOI of 0.5 alone or with 1 nM rapamycin or 100 μM TMZ over 72 h as described previously.[9] MOI, multiplicity of infection; TMZ, temozolomide.

(7.0–12) days; $P<0.001$), but RAD001-treated mice did not (mean survival = 27.5 vs 30.5 days; difference = 4 (−1 to 9) days; $P=0.14$). Strikingly, mice treated with OBP-405 and TMZ survived significantly longer than those treated with TMZ alone (mean = 53.0 vs 37.0 days; difference = 15.1 (7.2–23.1) days; $P=0.0015$), and mice treated with OBP-405 and RAD001 survived significantly longer than those treated with RAD001 alone (mean = 38.0 vs 30.5 days; difference = 9.3 (1.7–16.8) days, $P=0.021$). Finally, compared with results using OBP-405 alone, the survival time of mice was significantly prolonged by combination with TMZ (difference = 19 (11–26) days, $P=0.0001$) or RAD001 (difference = 7 (1–13) days, $P=0.025$).

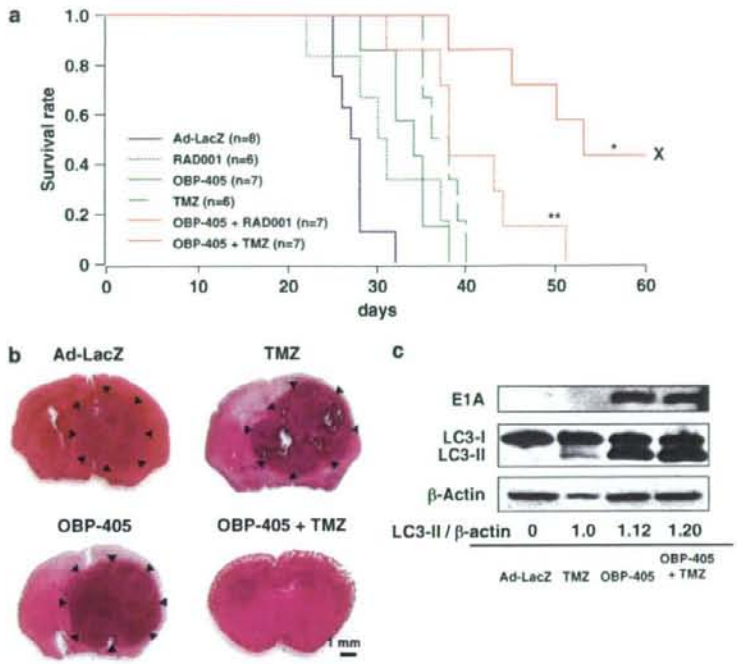

Figure 5 (**a**) Curves showing overall survival of mice bearing U87-MG intracranial tumors treated with Ad-LacZ, RAD001, TMZ, OBP-405, OBP-405 plus RAD001 or OBP-405 plus TMZ. The Kaplan–Meier method and pooled-variance two-tailed *t*-test were used to assess the statistical significance of differences in survival time; $^{*}P = 0.0015$ vs TMZ; $^{**}P = 0.021$ vs RAD001; 8- to 12-week-old female nude mice (Department of Experimental Radiation Oncology, MD Anderson Cancer Center) were used. The intracranial tumor model using U87-MG cells (5×10^5) was established as described previously.[3] Three days after the inoculation of U87-MG cells (day 0), the treatments were initiated as follows. On days 3, 5 and 7, through a 10 μl Hamilton syringe fitted with a 26-gauge needle connected to a microinfusion pump, Ad-LacZ (2.2×10^9 pfu ml^{-1}) or OBP-405 (2.2×10^9 pfu ml^{-1}) in 10 μl of sterile PBS was infused into the tumors through the screw guide at a depth of 3.5 mm from the skull. Two hundred microliters of TMZ (7.5 mg kg^{-1} in PBS with 5% dimethyl sulfoxide) was injected intraperitoneally five times a week for 2 weeks, and RAD001 (5 mg kg^{-1} in water, kindly supplied by Norvartis, Basel, Switzerland) was administered orally every day until the animals became moribund and were killed. (**b**) Hematoxylin and eosin-stained brain tissues of mice bearing intracranial U87-MG tumors treated with Ad-LacZ (day 32), TMZ (day 40), OBP-405 (day 38) or OBP-405 plus TMZ (day 60). Scale bar = 1 mm. (**c**) Western blots showing induction of autophagy and expression of E1A in intracerebral tumors treated with Ad-LacZ (day 28), TMZ (day 39), OBP-405 (day 35) or OBP-405 plus TMZ (day 53). Anti-LC3B antibody and anti-E1A antibody were used. The intensities of the amount of LC3-II bands were normalized by the bands' intensities of β-actin. PBS, phosphate-buffered saline; TMZ, temozolomide.

The intracranial tumors of mice treated with Ad-LacZ, OBP-405, TMZ or RAD001 alone grew extensively, with midlines shifted laterally. Strikingly, tumors were undetectable in brain tissue harvested from three mice treated with OBP-405 plus TMZ that survived 60 days after inoculation (Figure 5b). Hexon was detected in the intracranial tumor treated with OBP-405 plus TMZ (day 45) but not in the tumor treated with Ad-LacZ (day 28) (Supplementary Figure 7). This finding was supported by western blotting results showing detectable E1A protein expression in intracranial tumors treated with OBP-405 alone or with TMZ (Figure 5c). These results indicated that OBP-405 replicated and spread through the intracranial tumors but not through the normal brain tissues and supported the contention that the effect of OBP-405 is specific to tumors, likely due to the hTERT promoter activity. Then, we determined whether the induction of autophagy is detected under *in vivo* settings using an anti-LC3B-specific antibody. As shown in Figure 5c, the amount of LC3-II was higher in intracranial tumors of mice treated with TMZ, OBP-405 and OBP-405 plus TMZ than in Ad-LacZ-treated mice. These results indicated that autophagy was induced in intracranial tumors of mice as well as *in vitro* and that the extent of autophagy was enhanced by the combination treatment. However, intracranial tumors established from noninvasive glioblastoma cell lines may limit the clinical relevance of studies assessing the efficacy of novel therapies.[21] Therefore, we will further assess whether the treatment with OBP-405 plus TMZ or RAD001 prolong the survival of the mice carrying invasive intracranial tumors.[21]

In conclusion, we found that the fiber-modified hTERT-Ad OBP-405 has a marked antitumor effect on glioblastoma cells regardless of the cellular expression level of CAR. Moreover, autophagy-inducing agents (TMZ and rapamycin) increase the *in vitro* and *in vivo* antitumor activity of OBP-405 through the enhancement of autophagic pathway. A recent clinical study showed that TMZ had antitumor activity both as a single agent

and as adjuvant chemotherapy for patients with malignant gliomas, although its efficacy was modest.[22] Our study results might indicate a new way to treat glioblastomas with a combination of autophagy-inducing agents.

Acknowledgements

We thank Dr Noboru Mizushima for the GFP-LC3 expression vector and the wild-type and *Atg5−/−* MEFs. We also thank E Faith Hollingsworth for technical support and Elizabeth L Hess for editing the manuscript. This work was supported in part by Grant CA-088936 from the National Cancer Institute (to S Kondo), by a generous donation from the Anthony D Bullock III Foundation (to Y Kondo, R Sawaya and S Kondo) and the Institutional Core Grant CA-16672 High Resolution Electron Microscopy Facility, MD Anderson Cancer Center.

Grant support: This study was supported in part by National Cancer Institute Grants CA088936 and CA108558, a start-up fund from The University of Texas MD Anderson Cancer Center (SK), a generous donation from the Anthony D Bullock III Foundation (YK, RS and SK) and the cancer center support grant (CCSG)/shared resources of MD Anderson Cancer Center.

References

1 Mathis JM, Stoff-Khalili MA, Curiel DT. Oncolytic adenoviruses-selective retargeting to tumor cells. *Oncogene* 2005; **24**: 7775–7791.
2 Ko D, Hawkins L, Yu DC. Development of transcriptionally regulated oncolytic adenoviruses. *Oncogene* 2005; **24**: 7763–7774.
3 Ito H, Aoki H, Kühnel F, Kondo Y, Kubicka S, Wirth T *et al*. Autophagic cell death of malignant glioma cells induced by a conditionally replicating adenovirus. *J Natl Cancer Inst* 2006; **98**: 625–636.
4 Ogier-Denis E, Codogno P. Autophagy: a barrier or an adaptive response to cancer. *Biochim Biophys Acta* 2003; **1603**: 113–128.
5 Gozuacik D, Kimchi A. Autophagy as a cell death and tumor suppressor mechanism. *Oncogene* 2004; **23**: 2891–2906.
6 Kondo Y, Kanzawa T, Sawaya R, Kondo S. The role of autophagy in cancer development and response to therapy. *Nat Rev Cancer* 2005; **5**: 726–734.
7 Wickham TJ, Mathias P, Cheresh DA, Nemerow GR. Integrins $\alpha_v\beta_3$ and $\alpha_v\beta_5$ promote adenovirus internalization but not virus attachment. *Cell* 1993; **73**: 309–319.
8 Hedley SJ, Chen J, Mountz JD, Li J, Curiel DT, Korokhov N *et al*. Targeted and shielded adenovectors for cancer therapy. *Cancer Immunol Immunother* 2006; **55**: 1412–1419.
9 Taki M, Kagawa S, Nishizaki M, Mizuguchi H, Hayakawa T, Kyo S *et al*. Enhanced oncolysis by a tropism-modified telomerase-specific replication-selective adenoviral agent OBP-405 ('Telomelysin-RGD'). *Oncogene* 2005; **24**: 3130–3140.
10 Klionsky DJ, Cuervo AM, Seglen PO. Methods for monitoring autophagy from yeast to human. *Autophagy* 2007; **3**: 181–206.
11 Paglin S, Hollister T, Delohery T, Hackett N, McMahill M, Sphicas E *et al*. A novel response of cancer cells to radiation involves autophagy and formation of acidic vesicles. *Cancer Res* 2001; **61**: 439–444.
12 Mizushima N. Methods for monitoring autophagy. *Int J Biochem Cell Biol* 2004; **36**: 2491–2502.
13 Mizushima N, Yoshimori T. How to interpret LC3 immunoblotting. *Autophagy* 2007; **3**: 542–545.
14 Aoki H, Takada Y, Kondo S, Sawaya R, Aggarwal BB, Kondo Y. Evidence that curcumin suppresses the growth of malignant gliomas *in vitro* and *in vivo* through induction of autophagy: role of Akt and extracellular signal-regulated kinase signaling pathways. *Mol Pharmacol* 2007; **72**: 29–39.
15 Aoki H, Kondo Y, Aldape K, Yamamoto A, Iwado E, Yokoyama T *et al*. Monitoring Autophagy in Glioblastoma with Antibody against Isoform B of Human Microtubule-Associated Protein 1 Light Chain 3. *Autophagy* 2008; **4**: 467–475.
16 Klionsky DJ, Abeliovich H, Agostinis P, Agrawal DK, Aliev G, Askew DS *et al*. Guidelines for the use and interpretation of assays for monitoring autophagy in higher eukaryotes. *Autophagy* 2008; **4**: 151–175.
17 Tanida I, Minematsu-Ikeguchi N, Ueno T, Kominami E. Lysosomal turnover, but not a cellular level, of endogenous LC3 is a marker for autophagy. *Autophagy* 2005; **1**: 84–91.
18 Shintani T, Klionsky DJ. Autophagy in health and disease: a double-edged sword. *Science* 2004; **306**: 990–995.
19 Takeuchi H, Kondo Y, Fujiwara K, Kanzawa T, Aoki H, Mills GB *et al*. Synergistic augmentation of rapamycin-induced autophagy in malignant glioma cells by phosphatidylinositol 3-kinase/protein kinase B inhibitors. *Cancer Res* 2005; **65**: 3336–3346.
20 Kanzawa T, Germano IM, Komata T, Ito H, Kondo Y, Kondo S. Role of autophagy in temozolomide-induced cytotoxicity for malignant glioma cells. *Cell Death Differ* 2004; **11**: 448–457.
21 Giannini C, Sarkaria JN, Saito A, Uhm JH, Galanis E, Carlson BL *et al*. Patient tumor EGFR and PDGFRA gene amplifications retained in an invasive intracranial xenograft model of glioblastoma multiforme. *Neuro Oncol* 2005; **7**: 164–176.
22 Stupp R, Mason WP, van den Bent MJ, Weller M, Fisher B, Taphoorn MJ *et al*. Radiotherapy plus concomitant and adjuvant temozolomide for glioblastoma. *N Engl J Med* 2005; **352**: 987–996.

Supplementary Information accompanies the paper on Gene Therapy website (http://www.nature.com/gt)